Hao Yu[1], Richard Coffin[1], Hannah Organ[1] and Derry Xu[1]

[1]Department of Physical and Environmental Sciences, Texas A&M University-Corpus Christi, Corpus Christi, Texas, USA.

Corresponding author: Hao Yu (hyu2@islander.tamucc.edu)

Key Points:

- CH_4 emission from sediment to water column was controlled by photosynthesis and respiration of seagrass in the subtropical lagoon.
- The tidal process affected CH_4 transport in the subtropical mangrove creek and decreased the potential of CH_4 emission to the atmosphere.
- Unlike those in the sediment-water interface, the CH_4 flux at the water-air interface was primarily influenced by wind speed.

Abstract

Seagrasses and mangroves are crucial sources of atmospheric methane (CH_4) from coastal areas. To study the dynamics of CH_4 cycling at subtropical seagrass and mangrove, we studied diurnal CH_4 emissions at the sea-air and sediment-water interfaces and related environmental parameters in August 2019 at lagoonal estuaries of southern Texas, USA, northwest coast of the Gulf of Mexico. Although seagrass meadows and mangroves locate at closely connected subtropical estuaries, they displayed distinct mechanisms in CH_4 cycling. Dissolved CH_4 concentration at the seagrass meadow decreased in the daytime and increased overnight, expressing a tight relationship with photosynthesis and respiration of seagrass. Plant mediation of seagrass played a crucial role in CH_4 production, oxidation, and transport from sediment to water column. In comparison, the diel variation of dissolved CH_4 concentration at the mangrove creek was controlled by tidal progression. The maximum CH_4 level occurred during ebb due to the export of CH_4 from inside the mangrove to the outside bay. Tidal pumping and tidal inundation were essential conduits for dissolved CH_4 exchange between water and porewater. In both areas, sea-air CH_4 fluxes were significantly affected by wind speeds, which hid related diurnal variations caused by physiological or tidal cycles. Our study also revealed a more significant contribution from seagrass to the local CH_4 budget than from mangroves, indicating CH_4 released from subtropical seagrass needs further investigation.

Plain Language Summary

CH_4 is the second important greenhouse gas after carbon dioxide (CO_2), but its warming potential is over 80 times that of CO_2. Coastal vegetation areas such as seagrass and mangrove are important natural sources of CH_4. Although the northwest coast of the Gulf of Mexico is essential seagrass and mangrove habitats, few studies have been concerned about the CH_4 emission from this region. This study investigated potential mechanisms that control diurnal CH_4 emission from the seagrass meadow and mangrove creek in southern Texas estuaries. We found that the CH_4 released from sediment to water in seagrass was influenced by seagrass photosynthesis and respiration. While in the mangrove creek, CH_4 variation in water was affected by the tidal process. Unlike the CH_4 flux in the sediment-water interface, the emission of CH_4 from water to the atmosphere was strongly controlled by wind speed in both seagrass and mangrove areas. Moreover, more CH_4 was released from seagrass to the air than from mangroves in these subtropical estuaries, suggesting more concern on seagrass CH_4 contribution.

1 Introduction

Coastal vegetated ecosystems such as mangroves, saltmarsh, and seagrass are a huge blue carbon reservoir, a crucial global carbon sink (Macreadie et al., 2019). The high deposition of organic carbon to these systems provides plenty of carbon sources for microbial production and subsequent respiration, leading to a high potential of greenhouse gas emission (Macreadie et al., 2019; Rosentreter et al., 2018). Results show that mangroves, salt marshes, and seagrasses are net CH_4 sources globally, with a total emission of 0.33~0.39 Tmol CH_4/year (5.3~6.2 Tg CH_4/year) (Al-Haj & Fulweiler, 2020). Combining these systems accounts for most CH_4 emissions from coastal and open oceans (4-10 Tg CH_4/yr with a mean of 6 Tg CH_4/yr) (Saunois et al., 2020; Weber et al., 2019).

Due to extensive spatial and temporal heterogeneity, CH_4 budgets from different vegetated origins are poorly constrained. For example, diurnal variations in CH_4 fluxes have been reported in some coastal vegetated areas. Maximum CH_4 emission could occur during night (Diefenderfer et al., 2018), in the daytime (Huang et al., 2019; Yang et al., 2018), or highly variable (Jha et al., 2014), or no significant diel pattern (Garcias-Bonet & Duarte, 2017; Li et al., 2018).

Diurnal variations of CH_4 emission have been reported to primarily result from short-term changes of hydrological and biogeochemical processes, such as tides and oxygen cycling mediated by photosynthesis and plant mediation. Sometimes, these processes could also work together (Maher et al., 2015) and sometimes competed with each other (Yang et al., 2018). In tidal-dominated coastal areas, tidal processes often significantly impact CH_4 emissions through water or porewater exchange (Li et al., 2018; Trifunovic et al., 2020). CH_4 fluxes in mangrove creeks have been observed higher in low tides due to tidally driven porewater exchange, or progressive enrichment of diffusive CH_4 in the water column (Call et al., 2015; Jacotot et al., 2018). Tidal inundation during spring tides also can release more CH_4 from intertidal sediment (Bahlmann et al., 2015; Call et al., 2019; Dutta et al., 2015). Drivers of CH_4 exchange between porewater and water column could be explained by ”lunar mangrove pump” and ”first-flush” in micro-tidal (Call et al., 2015) and macro-tidal (Call et al., 2019) mangrove systems, respectively. In riverine estuaries, tidal-fluvial interaction on ecosystem metabolism could regulate CH_4 dynamics (Huertas et al., 2018; Matoušů et al., 2017). Tidally controlled CH_4 variation was also reported at the seagrass meadow of Ria Formosa lagoon (southern Portugal) (Bahlmann et al., 2015).

Transport of photosynthetic oxygen to plant roots could promote aerobic CH_4 oxidation and/or influence CH_4 production by changing sediment redox conditions. Many studies have displayed CH_4 oxidation in the rhizosphere of macrophytes (Heilman & Carlton, 2001; Kankaala & Bergström, 2004; Lombardi et al., 1997). A study at seagrass meadows and coral reefs in Caesar Creek, Florida, suggested the impact of photosynthetic oxygen on CH_4 production rate in sediment (Oremland, 1975). Diel variations of O_2, N_2, and CH_4 in sediment bubbles and rhizome gases in seagrass *T. testudinum* manifested that O_2 produced during photosynthesis could be delivered via the rhizome system to sediment, and it was negatively related to CH_4 proportions (Oremland & Taylor, 1977). Although oxygen cycling is crucial to seagrass physiology, few studies systematically investigated how photosynthetic processes influence CH_4 emission from seagrass meadows.

Oxygen cycling in vegetation areas is tightly related to the mediation capability of plants. Plant mediation can transport oxygen and deliver all other gases, including CH_4 (Oremland & Taylor, 1977). Plant-mediated transport of CH_4 has been observed in many emergent and submerged macrophytes (Chanton et al., 1992; Fonseca et al., 2017; Laanbroek, 2009; Whiting & Chanton, 1992; Zhang et al., 2019). Mangroves also have been found to have the plant-mediation capability in CH_4 transport, with CH_4 emission from stems positively correlated with the number of mangrove pneumatophores (Jeffrey et al., 2019; Livesley & Andrusiak, 2012). Even though there has not been direct evidence to show the transport of CH_4 through seagrass' aerenchyma, CH_4 had been observed in the rhizomatic internal structure of some seagrass (Oremland & Taylor, 1977).

CH_4 emission to the atmosphere from shallow coastal areas depends on all periods of CH_4 biogeochemical cycling, including CH_4 production, oxidation, and transport (Figure 1). CH_4 is primarily produced from anaerobic methanogenesis and can be oxidized by methanotrophic sediment and water column cycling or with sunlight penetration photo-oxidation. CH_4 not oxidized through these cycles could finally be transported to the atmosphere. Although long-term observation approaches such as the eddy covariance technique and chambers integrated with continuous measurement are robust in capturing the diurnal variation in CH_4 fluxes to the atmosphere (Huang et al., 2019; Jha et al., 2014; Li et al., 2018; Yang et al., 2018), only a systematic study integrate CH_4 transport from sediment to water and from water to air can discover the mechanisms and factors controlling CH_4 emission to the air.

This study investigated diurnal variation in CH_4 and other parameters in seagrass and a mangrove creek in adjacent estuaries at the northwest Gulf of Mexico. Although northwest coasts of the Gulf are essential mangrove and seagrass habitats, CH_4 released from this region has few studies. Most studies focused on the eastern and southern coasts of the Gulf (Cabezas et al., 2018; Chuang et al., 2017; Oremland, 1975; B. J. Wilson et al., 2015). Mangrove forests at Aransas Bay, Texas, are one of the key areas of northward mangrove expansion and replacement of salt marsh along the Gulf, with mangrove coverage increased

75% between 1990 to 2010 (Armitage et al., 2015; Osland et al., 2018). The transfer from salt marsh to mangrove could deposit more carbon in the sediment (Bianchi et al., 2013) and bring the potential for more CH_4 emission. Locating at the south of Port Aransas, Laguna Madre is one of the most hypersaline lagoons in the world. It is dominated by seagrass, particularly *Halodule wrightii*, a pioneer species with a tolerance of high salinity (Wilson & Dunton, 2018).

In this study, we systematically observed the photosynthesis-related CH_4 transport in a subtropical seagrass meadow and tide-driven CH_4 cycling in a mangrove creek. This study uncovers mechanisms that control the diurnal CH_4 transport from sediment to water and from water to atmosphere of these two different vegetation systems, and quantitively determined CH_4 variation in different periods during the diurnal observation. Comparing CH_4 cycling in adjacent mangrove and seagrass systems was expected to understand the coastal wetland CH_4 emissions further. This study also supplements sparse methane data along the Gulf of Mexico and provides a more thorough understanding for CH_4 cycling in subtropic areas.

2 Materials and Method

2.1 Study area

This study is in a semi-tropical zone, in the northwest of the Gulf of Mexico, southeast coast of Texas, including southern Aransas Bay (Harbor Island) and Upper Laguna Madre (Figure 1). The estuaries are separated from the Gulf of Mexico by sandy barrier islands, Padre Island, Mustang Island, and San José Island, and only through the Packery Channel and the Ship Channel at Port Aransas can access water of the Gulf of Mexico. Dominated by diurnal microtides, these estuaries have a limited water exchange with the Gulf of Mexico (Smith, 1979).

Harbor Island is near the inlet of Ship Channel. It is covered by black mangrove (*Avicennia germinans*) and salt marsh (*Spartina alterniflora* and other grass and forb species) (Armitage et al., 2015). From the 1930's to the present, the coverage of black mangroves at Harbor Island had a notable increase, and salt marsh decreased significantly (Armitage et al., 2015; Montagna et al., 2011). It has become one of the primary populations of black mangroves on the Texas coast (Montagna et al., 2011). Upper Laguna Madre is the northern part of Laguna Madre, one of three hypersaline lagoons globally. It is crucial seagrass habitat, with seagrass meadow covering approximately 66% of the floor (Dunton & Reyna, 2019). *H. wrightii* (56.0 ± 39.1%, 2018) dominated the region, followed by *S. filiforme* (9.2 ± 23.1%, 2018) and *H. engelmannii* (0.5 ± 4.7%, 2018) (Dunton & Reyna, 2019). The whole study area, whatever is dominated by seagrass, salt marsh and/or mangrove habitats, provides vital nursery habitat to many birds, fish, and invertebrate species. It also serves as a major area for public recreation, e.g., boating and fishing.

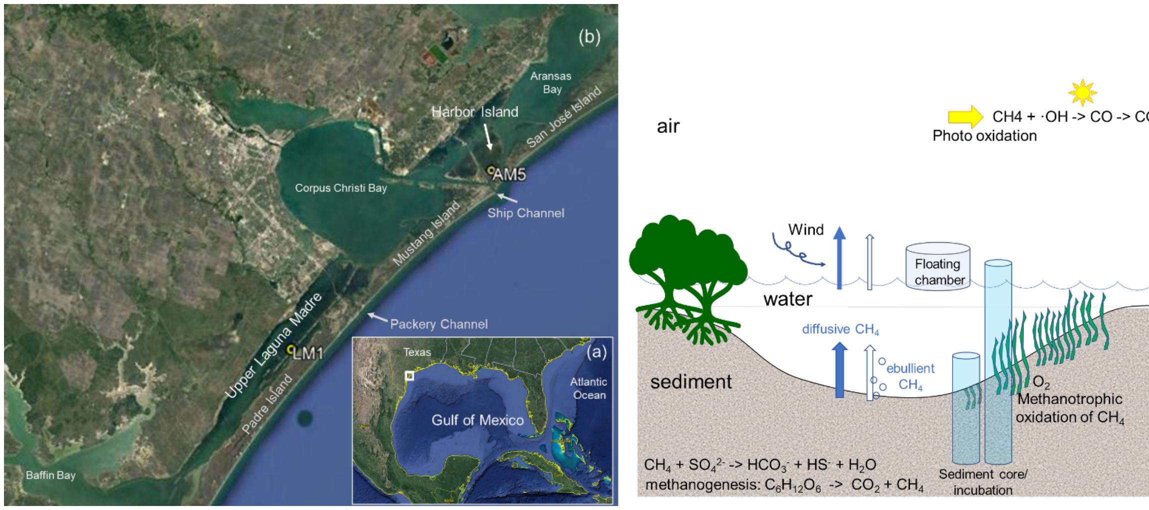

Figure 1. Study area and method. Left: (a) An overview of the Gulf of Mexico. The study area is located northwest of the Gulf of Mexico and southeast of Texas, USA, marked by the white rectangle. (b) Sampling sites. AM5 locates at a creek of Harbor Island; LM1 locates in the middle of Upper Laguna Madre. Right: Scheme of CH4 cycling and study approaches.

2.2 Study method and sampling

Diurnal observation and sampling were carried out at the site LM1 (27°32'39.16"N, 97° 17'9.5"W, seagrass) of Upper Laguna Madre on August 13th and 14th, 2019, and at AM5 (27°51'54.85"N, 97° 3'35.91"W, mangrove) of Harbor Island on August 15th and 16th, 2019 (Figure 1). To thoroughly understand transport of methane from sediment to the atmosphere via water column, we investigated CH_4 emissions at both the water-air and sediment-water interfaces.

Surface water and ambient air samples were collected every 4 hours to determine a 24-hour variation of dissolved CH_4, sea-air CH_4 flux, dissolved inorganic carbon (DIC), and Chlorophyll-*a* (Chl-*a*). Synchronically, water parameters (salinity, pH, dissolved oxygen (DO), temperature) were measured using a multiparameter meter (HI98194, Hanna Instruments). Air temperature and wind speed were measured by a portable anemometer positioned 1m above the surface water. Daily wind speed and hourly temperature, and wind speed data were acquired online (NOAA National Centers for Environmental Information Climate Data Online https://www.ncdc.noaa.gov/cdo-web/). These parameters were applied to calculate the CH_4 flux and analyze factors controlling CH_4 emission at the sea-air interface (Chuang et al., 2017; Lorenson et al., 2016). Floating chambers were set up at the same time to measure in-situ CH_4 flux from surface water to the atmosphere (Figure 1).

To determine CH_4 emission at the sediment-water interface, sediment cores were collected, and in-situ sediment chambers were established for sediment incubation experiments at LM1 and AM5. Porewater CH_4 profiles through sediment cores were applied to calculated diffusive CH_4 fluxes at the sediment-water surface. Variation of CH_4 in the overlying water of sediment chambers before and after incubation could indicate total sediment-water CH_4 fluxes during the experiment.

2.2.1 Surface water collection

For each site, surface water samples were overflowed three times the volume into 160 ml glass vials. Then 1 ml saturated $CuSO_4$ solution was added to inhibit microbial growth. Ambient air samples were collected at the same time for background CH_4 concentrations. Water and air samples were stored in the dark and measured within two months after they were collected. Water incubation experiments at LM1 and AM5 were used to measure the oxidation of CH_4 in water column by adding a saturated $CuSO_4$ solution to duplicate water samples in a certain interval.

2.2.2 Floating chamber observation

Floating chambers were placed at LM1 and AM5 to observe in-situ CH_4 flux at the water-air surface. Polyester bottles made floating chambers with a volume of 3 liters. In the first hour, air samples in floating chambers were collected every 15 minutes using a 30ml syringe and injected into the vial filled with Milliq water which had been purged with pure N_2. Then air inside chambers was sampled every 4 hours during the diurnal observation.

2.2.3 Sediment cores incubation experiment

Sediment cores were collected at LM1 and AM5 using 50cm polycarbonate tubing with 6.67cm of diameter. For each core, porewater samples were drawn with Rhizon samplers (Coffin et al., 2013) and 30 ml syringes immediately after the cores were collected at the interfere of 2 cm. Then porewater samples were transferred to 30 ml vials previously filled with pure N_2 gas, and 0.2ml saturated $CuSO_4$ solution was injected immediately, and then stored in dark and cool till measurement.

Sediment incubation experiments were carried out using 70cm polycarbonate tubing with 6.67cm of diameter. At LM1 and AM5, two sediment chambers were inserted into the sediment. One chamber was merged into water totally, and the upper opening was sealed, and the other was left headspace air and then sealed. They were fixed to stand up together at LM1 or AM5 for nearly 24 hours. After in-situ incubation, overlying water of each chamber and headspace air of chambers at LM1 and AM5 were collected using 60 mL glass vials and 30 ml vials, respectively. Porewater was sampled using the same method as porewater collection from sediment cores.

2.3 Analytical Methods

Concentrations of dissolved and airborne CH_4 were measured by the headspace equilibration technique and Gas Chromatograph (GC, Agilent 6890N) (Magen et al., 2014; Reeburgh, 2007). DIC concentrations were determined using UIC CM5017 Coulometer. Chlorophyll *a* (Chl-*a*) concentrations were measured using Turner 10-AU. Sulfide in porewater was determined by colorimetric analysis of the methylene blue method (Cline, 1969; Reese et al., 2011). The above works were done in the Isotope Core Laboratory at Texas A&M University-Corpus Christi. $^{13}C\text{-}CH_4$ of some samples were analyzed at the Stable Isotope Lab of the University of California-Davis.

Diffusive CH_4 flux in the sea-air interface was calculated using the Gas-transfer Model (Wanninkhof, 1992).

$J = k_v \cdot (C_{obs} - C_{eq})$ (1)

Where, J is the flux of gas to the atmosphere ($mmol \cdot m^{-2} \cdot d^{-1}$ or $\mu mol \cdot m^{-2} \cdot h^{-1}$); C_{obs} represents the measured concentration of dissolved CH_4 in water ($nmol \cdot L^{-3}$); C_{eq} is the concentration of CH_4 in equilibrium with the atmosphere at in situ temperature ($nmol \cdot L^{-3}$), calculated for each sample from the temperature- and salinity-dependent equilibrium relationship (Wiesenburg & Guinasso, 1979); k_v is gas transfer velocity ($m \cdot d^{-1}$), calculated using the relationship between gas transfer and wind speed developed and updated by Wanninkhof in 1992 and 2014 (Wanninkhof, 1992, 2014). Based on the comparison between calculated diffusive fluxes and CH_4 fluxes got using floating chambers, this study used the coefficient of 0.251 in calculating k_v. That is, $k_v = 0.251 \times \mu^2 \times (\frac{Sc}{660})^{-\frac{1}{2}}$ (Wanninkhof, 2014).

Sea-air CH_4 flux ($\mu mol \cdot m^{-2} \cdot h^{-1}$ or $mmol \cdot m^{-2} \cdot d^{-1}$) acquired using floating chambers, which is called chamber flux in this paper, was calculated from the variation of CH_4 proportion in the chambers during in-situ observation.

Dissolved CH_4 flux at the sediment-water interface was calculated using Fick's First Law (Berner, 1980).

$J_s = -\emptyset \left(D_0 \bullet \theta^{-2}\right) \left[\frac{dc}{dz}\right]$ (2)

J_s is the diffusive CH_4 flux at the sediment-water surface; $\emptyset$ is the porosity of sediment, measured from the weight loss of sediment dried at 80°C (Morin & Morse, 1999); D_0 is diffusion coefficient for CH_4 in water ($1.5 \times 10^{-5}\ cm^2 \cdot s^{-1}$) (Broecker & Peng, 1974); θ is tortuosity, calculated using $\theta^2 = 1 - ln\left(\emptyset^2\right)$ (Boudreau, 1996); $\frac{dc}{dz}$ is CH_4 gradient in porewater. Both the gradient of the first two layers of porewater and the gradient between bottom water and first layer of porewater were applied to represent sediment-water CH_4 fluxes.

3. Results

3.1 Diurnal variation of dissolved CH_4 and other parameters

Diurnal observations found dissolved CH_4 concentration in seagrass site LM1 decreased and reached the lowest before the sunset, while overnight CH_4 concentration increased and arrived at highest before sunrise (Figure 2 left: a, c, e). Such variation of dissolved CH_4 concentration had a similar trend with DIC and was the opposite of pH, Chl-*a*, DO, water level, temperature, and wind speed. The change of water level during the observation was minor, with no more than 0.02 meters. ^{13}C-CH_4 in water was -57.8‰ ~ -57.3‰, indicating its biogenic origin. Hourly diffusive CH_4 fluxes had a similar trend with hourly average wind speed. (Figure 2: g). Wind speed decreased from evening to dawn, and so did CH_4 flux and atmospheric CH_4 concentration, although dissolved CH_4 concentration increased. Before sunrise, although CH_4 concentration was the peak, CH_4 flux and atmospheric CH_4 proportion were lowest.

Diurnal variations in dissolved CH_4 concentration and other parameters in the mangrove area (AM5, Figure 2 right: b, d, f) were quite different from those in seagrass. Dissolved CH_4 concentration increased from noon, and reached the highest level at midnight, and then decreased. Such change was opposite to water level and DO concentration, but consistent with salinity and DIC. In comparison with that at LM1, there was significant variation in water level due to tidal processes. ^{13}C-CH_4 were -61.9‰ ~ -60.9‰, suggesting a biogenic CH_4 source. Sea-air CH_4 fluxes were corresponding with wind speed. Similar to LM1, wind speed decreased from late afternoon to dawn, and so did CH_4 flux. Even though dissolved CH_4 concentration was highest in the middle night, sea-air CH_4 flux was low due to slow wind speed.

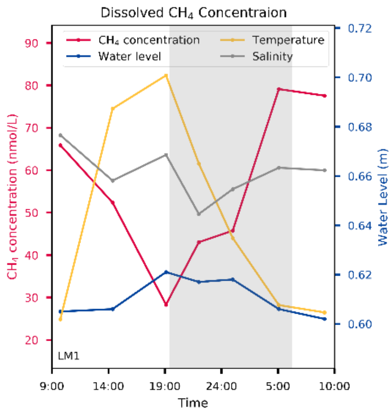
Dissolved CH4 Concentraion
CH4 concentration
Water level
Temperature
Salinity
CH4 concentration (nmol/L)
Water Level (m)
Temperature (°C)
LM1
Time

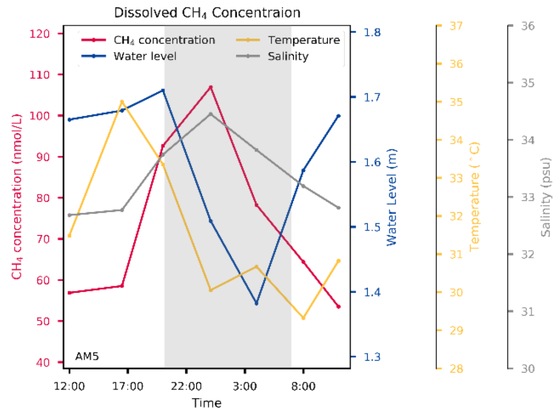
Dissolved CH4 Concentraion
CH4 concentration
Water level
Temperature
Salinity
CH4 concentration (nmol/L)
Water Level (m)
Temperature (°C)
Salinity (psu)
AM5
Time

(b)

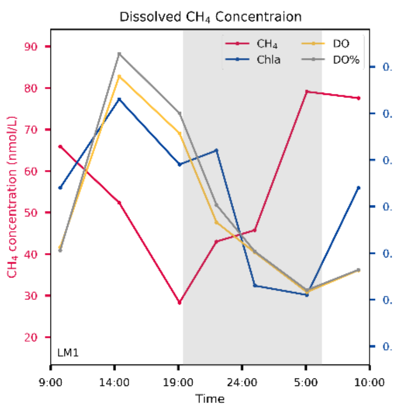
Dissolved CH4 Concentraion
CH4
Chla
DO
DO%
CH4 concentration (nmol/L)
Chla (ug/L)
LM1
Time

(c)

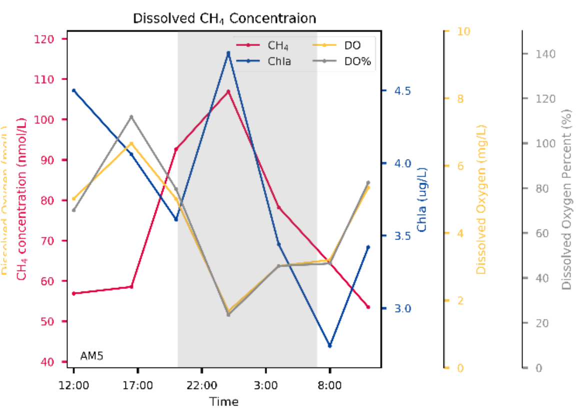
Dissolved CH4 Concentraion
CH4
Chla
DO
DO%
CH4 concentration (nmol/L)
Chla (ug/L)
Dissolved Oxygen (mg/L)
Dissolved Oxygen Percent (%)
AM5
Time

(d)

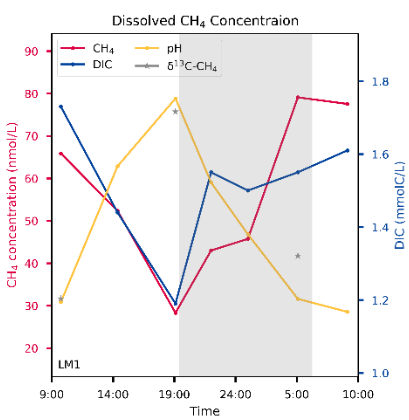
Dissolved CH4 Concentraion
CH4
DIC
pH
δ13C-CH4
CH4 concentration (nmol/L)
DIC (mmolC/L)
LM1
Time

(e)

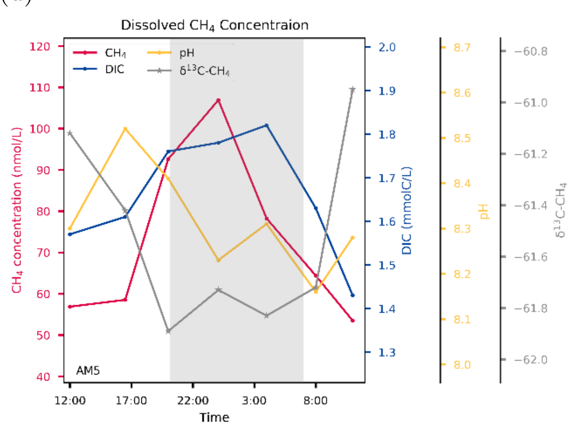
Dissolved CH4 Concentraion
CH4
DIC
pH
δ13C-CH4
CH4 concentration (nmol/L)
DIC (mmolC/L)
pH
δ13C-CH4
AM5
Time

(f)

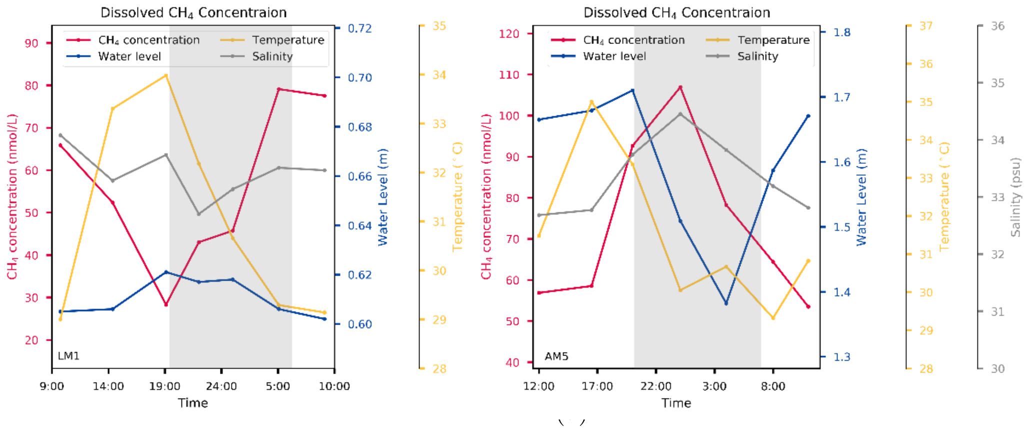

(b)

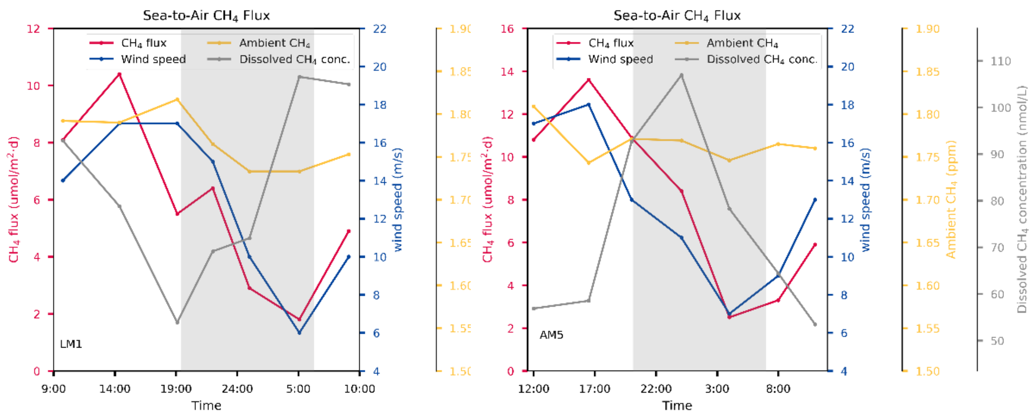

(g) (h)

Figure 2. Diurnal variation of dissolved CH_4 concentration and other parameters: (a) and (b) water level, temperature, and salinity; (c) and (d) Chl-*a* and DO; (e) and (f) DIC, pH and ^{13}C-CH_4; (g) and (h) hourly sea-air CH_4 flux, ambient CH_4 and wind speed; left: LM1, right: AM5.

3.2 Variation of CH_4 in floating chambers

Total CH_4 flux, both diffusive and ebullient, was measured by floating chambers. In one hour, variation of CH_4 in floating chambers increased linearly (Figure 3 a and b), indicating CH_4 entering the chambers were primarily diffusive in both seagrass and mangrove sites. Average growth rates of CH_4 proportion in chambers built in the daytime (0.020±0.010 ppm/min at LM1 and 0.0081±0.001 ppm/min AM5) were larger than those set up in the night (0.013 ppm/min at LM1 and 0.0058 ppm/min at AM5). It revealed that more CH_4 was released from water to the air in the daytime than at night. Moreover, the average CH_4 production rates in seagrass chambers were larger than in mangrove chambers.

For a 24-hour observation, CH_4 proportions in chambers did not increase linearly (Figure S1), which suggested CH_4 fraction in the gas entering chambers varied in the day-night cycle. This point also reflected from the variation of ^{13}C-CH_4 (Figure 3 c and d; LM1: -52.5‰ ~ -46‰; AM5: -58.6‰ ~ -46.4‰). Moreover, the ^{13}C-CH_4 values were negatively related to CH_4 proportions in both seagrass and mangrove sites (Figure 3 d and f).

Floating chamber fluxes in the first hour were similar with synchronous calculated diffusive flux at LM1 (Figure 3g), further implied no contribution from ebullition CH_4 and more significant daytime than nighttime emissions. Unlike at LM1, the first-hour floating chamber fluxes were lower than diffusive flux at AM5. It also manifested no ebullition CH_4 entering the chambers. Such a large discrepancy between floating chamber fluxes and diffusive flux indicated the impact of wind, which will be discussed later.

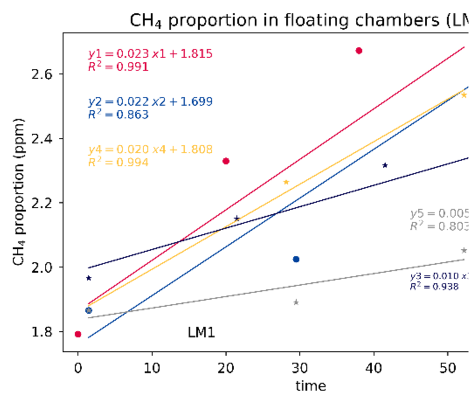

(a)

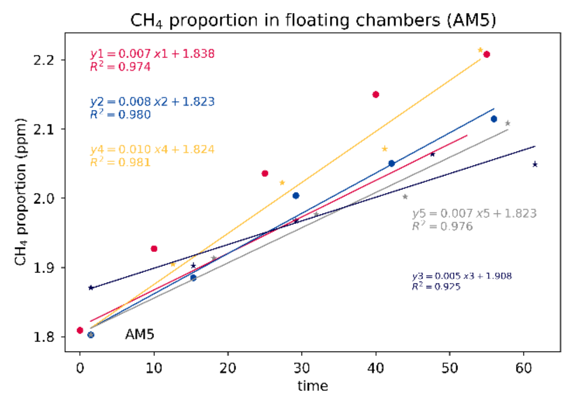

(b)

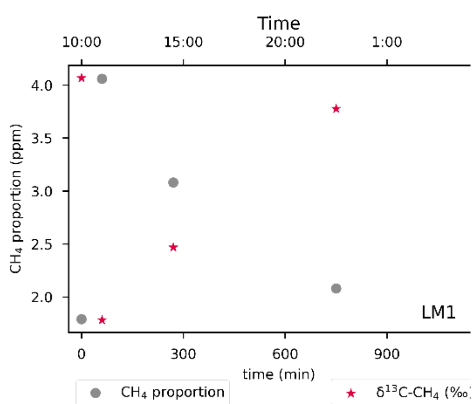

(c)

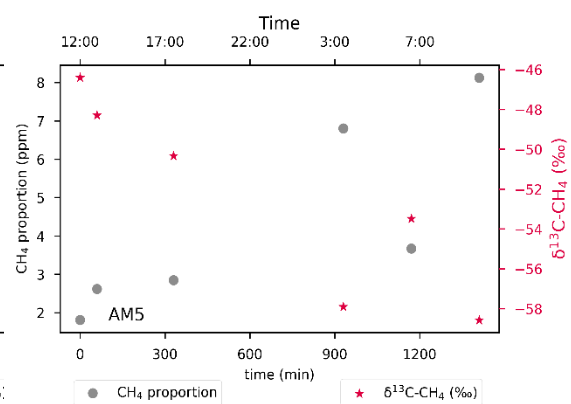

(d)

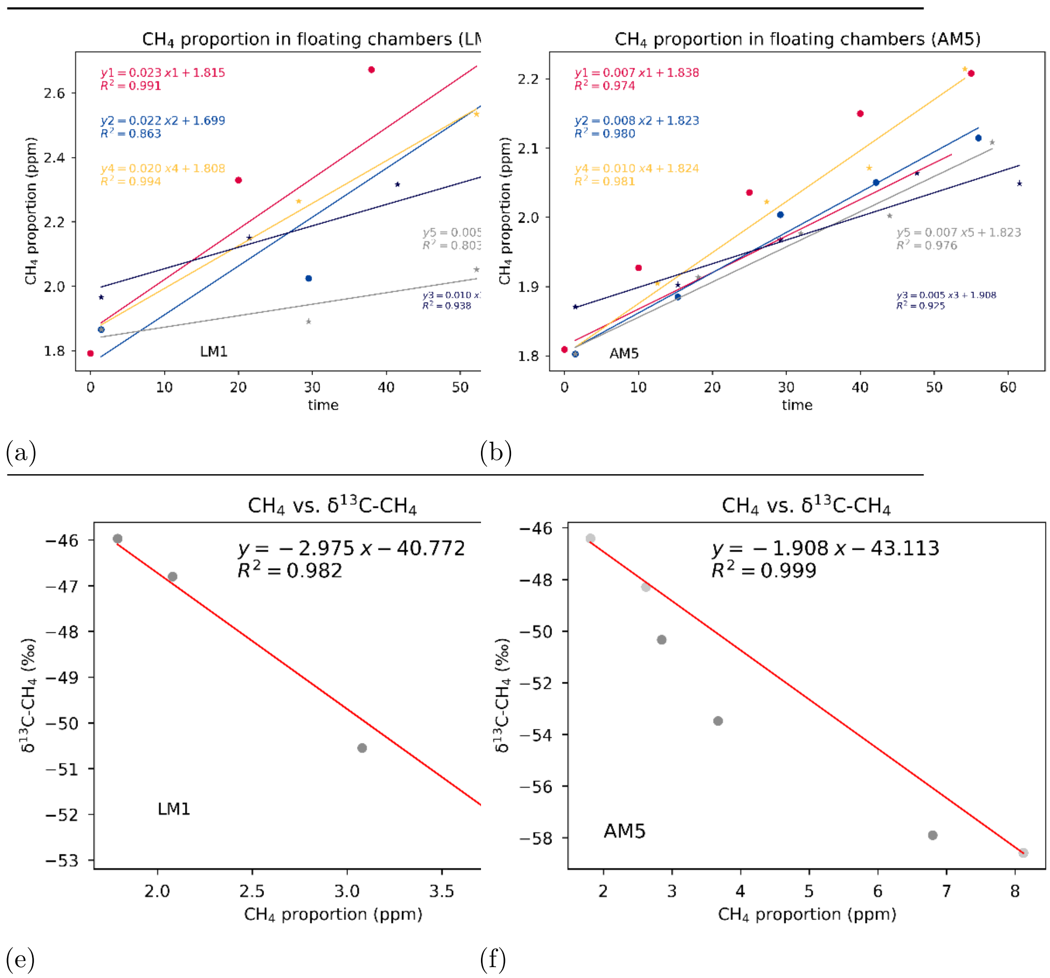

CH₄ proportion in floating chambers (LM
CH₄ proportion in floating chambers (AM5)
y1 = 0.023 x1 + 1.815
R² = 0.991
y2 = 0.022 x2 + 1.699
R² = 0.863
y4 = 0.020 x4 + 1.808
R² = 0.994
LM1
y1 = 0.007 x1 + 1.838
R² = 0.974
y2 = 0.008 x2 + 1.823
R² = 0.980
y4 = 0.010 x4 + 1.824
R² = 0.981
y5 = 0.007 x5 + 1.823
R² = 0.976
y3 = 0.005 x3 + 1.908
R² = 0.925
AM5
CH₄ proportion (ppm)
time
(a)
(b)
CH₄ vs. δ¹³C-CH₄
y = −2.975 x − 40.772
R² = 0.982
LM1
y = −1.908 x − 43.113
R² = 0.999
AM5
δ¹³C-CH₄ (‰)
CH₄ proportion (ppm)
(e)
(f)

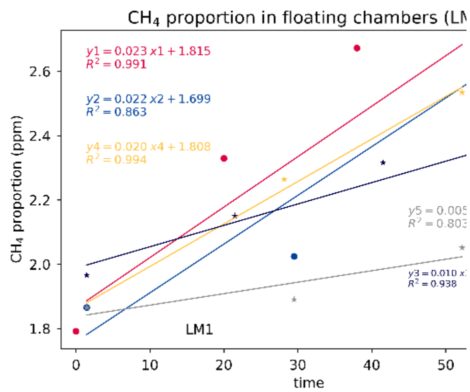

(a)

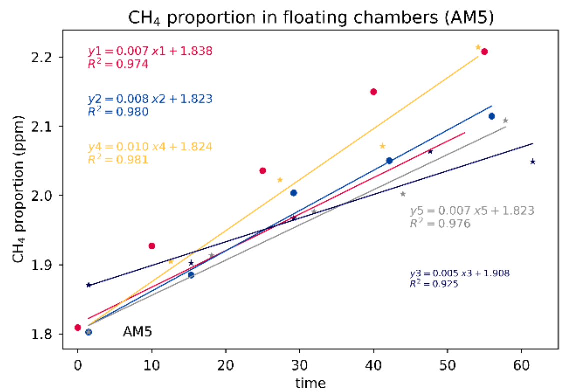

(b)

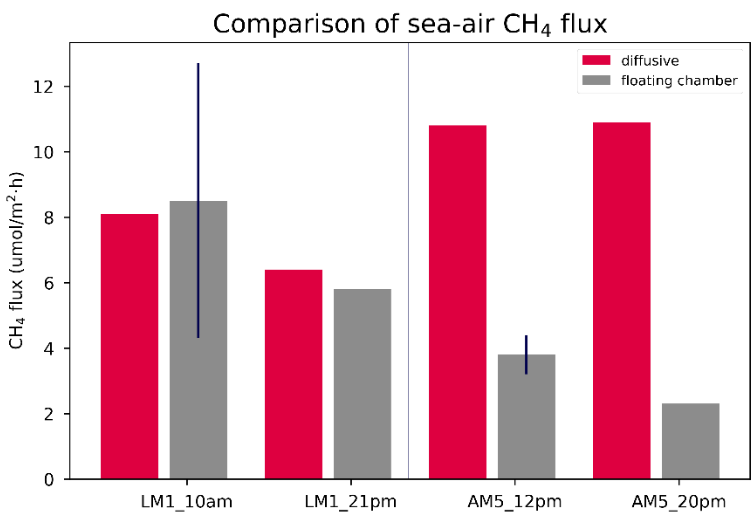

(g)

Figure 3. Floating chambers. (a) and (b) CH_4 proportion in floating chambers in the first hour at LM1 and AM5; (c) and (d) CH_4 proportion and ^{13}C-CH_4 in floating chambers in 24 hours; (e) and (f) CH_4 proportion vs. ^{13}C-CH_4 in floating chambers; (g) Comparison of calculated diffusive CH_4 fluxes and floating chamber fluxes

3.3 Sediment porewater and incubation

At the start of incubations, porewater CH_4 and sulfide concentrations were similar at LM1 (CH_4: 30 ~ 60 nmol/L; sulfide: 0~110µmol/L) and AM5 (CH_4: 20 ~ 90 nmol/L; sulfide: 0~110µmol/L) (Figure S2). After incubation, CH_4

concentrations in overlying water increased at the sediment chambers without headspace air (Figure 4a). The increase of CH_4 concentrations was larger in overlying water of seagrass site (LM1) and mangrove (AM5). Differently, in the chambers with headspace air, dissolved CH_4 concentrations decreased (Figure 4b), but CH_4 proportion in headspace air increased (Figure 4c). Moreover, the CH_4 amount entering air was larger than that decrease in the water column. Only a part of the elevated CH_4 in headspace could be explained by the decrease of CH_4 in water.

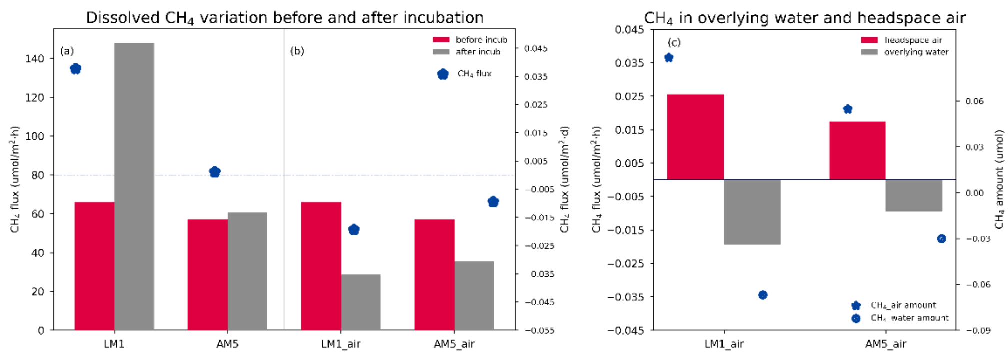

Figure 4. CH_4 variation in overlying water and headspace air in sediment incubation experiment. (a) Dissolved CH_4 concentration in overlying water in sediment chambers without headspace air; (b) Dissolved CH_4 concentration in overlying water in sediment chambers with headspace air; and (c) Variations of flux and amount of CH_4 in overlying water and headspace air after incubation in chambers with headspace air.

3.4 Water incubation

Maximum variations of dissolved CH_4 concentration in the incubation experiments were no more than 15% in 24 hours (Figure S3), indicating low bacterial water column consumption and production. Dissolved CH_4 concentration in samples collected at LM1 decreased 14% in the first hour and returned to 93% in the following 12 hours. Decrease of CH_4 concentration in AM5 samples occurred in the first four hours, and then CH_4 concentration returned and was stable at a bit over 90% in the following hours.

4. Discussion

4.1 CH_4 transport from sediment to water and air

Sediment-water CH_4 fluxes were calculated through two approaches. The first one is based on the variation of CH_4 concentration in overlying water of sediment chambers before and after incubation (Table 1). The second method uses Fick's first law of diffusion to calculate CH_4 flux at the sediment-water interface. Since CH_4 concentrations in the water column were less than those in top-layer porewater, the calculated diffusion fluxes were negative in both LM1 and AM5 (Table 1). The diffusion fluxes across top-layer and second-layer sediment were positive. But they were much less than the fluxes acquired using sediment incubation, indicating diffusive passage was not the primary path for CH_4 transport from sediment porewater to water column in the seagrass meadow and mangrove creek.

Moreover, incubation sediment-water flux was larger at LM1 than at AM5, while diffusive flux at LM1 was much less. It suggested more CH_4 was released from seagrass sediment to the water column than from mangrove sediment using a more robust transport approach. The CH_4 flux entering headspace air through water and/or sediment at LM1 was also larger than at AM5, further expressing this point.

In the sediment chambers with headspace air, CH_4 concentrations in overlying water decreased after incubation while concentrations in headspace air increased. The increased amounts of CH_4 in the headspace air (LM1: 0.088 µmol; AM5: 0.055 µmol) were larger than the decrease in overlying water (LM1: -0.067 µmol; AM5: -0.030 µmol) at both sites, suggesting some CH_4 in the air came from sediment. Before incubation, CH_4 in the surface water was oversaturated at both sites, with saturations over 3500% and 3100% at LM1 and AM5. After incubation, saturations at both sites decreased to 405% and 976%, respectively. Our water incubation experiments showed that CH_4 concentration decreased about 10% in 24 hours, which denied the possibility CH_4 was produced in water column and transported to the headspace air. Theses observations demonstrated a contribution of atmospheric CH_4 came from sediment.

Table 1

Sediment-water and Water-air CH_4 Fluxes

	Sediment-water flux (mmol/m^2 · d)		Sed-(water)-air (mmol/m^2 · d)	Environn
	Incubation Flux	Sed-water Ficks	Sed-water Ficks_interface[1]	
LM1	0.0377	5.180E-06	-3.804E-05	
LM1-air	-0.0194	-	-	
AM5	0.0011	0.000102	-0.000032	
AM5-air	-0.0095	0.000133	0.000518	

	Water-air CH_4 flux (mmol/m^2 · d)	Environment		
	Diffusive[2]	Floating chamber in situ[3]	Floating chamber final[4]	Floating c
LM1	0.144	0.0895	0.077±0.012	0.174
AM5	0.202	0.0514	0.053	0.075

[1] interface of water and the first layer of sediment porewater

[2] sum of sea-air diffusive fluxes at the different period during observation

[3] sum of floating chamber fluxes at the different period during observation

[4] based on the increase of CH_4 in the floating chamber at the end of observation

[5] total flux of multiplication of one-hour floating chamber fluxes at daytime and nighttime and duration (hours) of daytime and nighttime respectively

CH_4 fluxes at the water-air interfaces were determined in two ways, the gas-transfer model and chamber observation. Fluxes acquired by both methods were much higher than the sediment-water fluxes, indicating the emission of CH_4 from water to the air was larger than the sediment supply of CH_4 to the water column. Such a significant imbalance between sediment-water and water-air fluxes at both LM1 and AM5 manifested that direct diffusive CH_4 transport at the sediment-water interface could not be the primary conduit for CH_4 entering the water in the long term.

4.2 Mechanism of CH_4 transport in seagrass

4.2.1 Impact of photosynthetic and respiration processes on CH_4 cycling

The diurnal variations at LM1 suggested dissolved CH_4 concentrations at the seagrass area were related to photosynthesis and respiration of seagrass, which can be reflected from variations of DO, Chl-*a*, DIC concentrations, and pH. In the daytime, oxygen produced during photosynthesis (equation 3) can diffuse to surrounding water and sediment, which improves DO concentration in the water column. Although respiration can consume oxygen (equation 4), the amount is much lower than that produced by the photosynthetic process (Borum et al., 2007). However, in the dark, oxygen consumption by respiration dominants and consequently DO concentration in the water column decreases because the supply from seagrass reduces (Borum et al., 2007). In this study, DO concentration was highest in the afternoon when Chl-*a* concentration was highest (Figure 2), which indicated the highest photosynthesis. Then DO concentration decreased to the lowest before sunrise as photosynthesis declined and then disappeared overnight, which was suggested by dropping Chl-*a* concentrations. Through sunrise, DO concentration began to increase. Variation of CO_2 in photosynthesis and respiration can be implied by DIC coupling with pH (equation 5). Lowest DIC and highest pH appeared before sunset, and the highest DIC and lowest pH happened before sunrise, which agreed with the daily circulation that photosynthetic consumes CO_2 and respiration produces CO_2. Although watershed mineralogy and riverine runoff have been found as primary drivers in some southern Texas estuaries (Yao & Hu, 2017), Upper Laguna Madre receives less such influences since the water exchange is weak and local evaporation exceeds all freshwater input (Montagna et al., 2018). Similar diel curves of DIC and DO were reported at Laguna Madre in September 1996 due to weak tidal exchange and strong biological signal (Ziegler & Benner, 1998).

- photosynthetic process: light + CO_2 + H_2O -> $C_6H_{12}O_6$ + O_2 (3)
- respiration: $C_6H_{12}O_6$ + O_2 -> CO_2 + H_2O + ATP (4)
- DIC and CO_2: CO_2 + H_2O HCO_3^- + H^+ (5)

In the diel observation, maximum dissolved CH_4 concentration in water occurred before sunrise (79.1 nmol/L) was nearly three times of minimal concentration (28.3 nmol/L) before sunset. Such discrepancy vastly exceeded the oxidation and production of CH_4 in the water column (no more than 15%) shown in the water incubation experiment. Hence the transport of CH_4 from sediment probably contributed to this diurnal variation. However, direct diffusive CH_4 fluxes at the sediment-water interface were minor compared to CH_4 fluxes at the sea-air interface (Table 1), which suggested the supply of diffusive CH_4 was not a significant way for CH_4 in water body. On the other hand, CH_4 flux at the sediment-water interface was four orders of magnitude higher than the calculated diffusive flux. It indicated the role of seagrass plant-mediation on CH_4 transport from sediment to water. Since seagrass lacunae tissues could transport oxygen produced in photosynthesis from leaves to water and rhizome sediment (Borum et al., 2007; Oremland & Taylor, 1977), such internal conduits also can facilitate the release of sediment CH_4 to the water body. Although there was no direct evidence about seagrass' plant mediation on CH_4, plant-mediated transport of CH_4 has been observed in many emergent and submerged macrophytes (Chanton et al., 1992; Fonseca et al., 2017; Laanbroek, 2009; Whiting & Chanton, 1992; Zhang et al., 2019). Moreover, diffusive CH_4 delivery could also be influenced by macrophytes' photosynthesis (Ding & Cai, 2007; Whiting & Chanton, 1996).

Although incubation sediment-water flux (0.0377 mmol/$m^2 \cdot d$) at LM1 was ~22% to ~50% of sea-air fluxes (0.077 ~ 0.174 mmol/ $m^2 \cdot d$, Table 1) in this study, their difference was reasonable. Since sediment surface area was larger than water surface due to complicated seafloor landform, total amount of CH_4 released from sediment was probable enough to support the emission from water to the atmosphere. The capability of plant-mediation also depends on the biomass of seagrass. Due to the limitation in *in-situ* experiment, we did not account for the seagrass biomass in sediment chambers, which brought uncertainty in the estimation of plant-mediated CH_4 transport. Moreover, as the dying of seagrass during incubation and CH_4 concentration in overlying water increased, it is reasonable that seagrass' transport capability decreased, and so the incubation flux was probably less than the transport flux by living plants. As a result, although incubation sediment-water flux was less than water-air flux, it is still can reflect the plant mediation of seagrass on CH_4.

As shown in Figure 5, dissolved CH_4 concentration was strongly negative with DO concentration measured four hours before and synchronically positively related with DIC. It indicates that the variation of CH_4 concentration is associated with the physiologic process of seagrass. Since oxygen is delivered within seagrass lacunae primarily driven by passive diffusion from leaves to roots (Borum et al., 2007), it is reasonable that the lowest CH_4 concentration appeared four hours after the DO peak. That CH_4 concentration varied oppositely with DO concentration could be attributed to two factors, direct oxidation of CH_4 in the rhizosphere and change of CH_4 production caused by diel variation of anaerobic and aerobic sediment environment. Rhizospheric CH_4 oxidation has been observed in some macrophytes up to 65% (Heilman & Carlton, 2001; Kankaala & Bergström, 2004; Lombardi et al., 1997). If the difference between the maximum and minimal CH_4 concentration in this study was entirely caused by oxidation in the rhizosphere, oxidation could also be nearly 65%. Considering the maximum potential of 15% decomposition in the water column, CH_4 oxidation in diel could be around 50%. The ^{13}C-CH_4 of in water was -57.8‰ ~ -57.3‰ during diurnal observation (Figure 2c), indicating its biogenic source of CH_4 in the water diurnally. The highest ^{13}C-CH_4 appeared when dissolved CH_4 concentration was lowest, which seemed related to oxidation of CH_4. However, the variation between maximum and minimal was not considerable enough as robust evidence of oxidation.

Another possibility is CH_4 production reduced in the daytime due to less anoxic surface sediment caused by photosynthetic oxygen. Lee et al. (2000) had observed porewater sulfide in seagrass meadows at Lower Upper Laguna Madre and Corpus Christi Bay decreased in mid-day because of increasing photosynthetic produced oxygen in sediment (Lee & Dunton, 2000). It means the sediment became much less anoxic. Consequently, less CH_4 may be produced in the daytime. On the contrary, less oxygen could be delivered to sediment at night because of less DO concentration, which created an anoxic environment for CH_4 production overnight.

Diurnal variation in CH_4 proportions and ^{13}C-CH_4 in the floating chamber also manifested that from late morning to early night, the transport of CH_4 from water to air decreased (Figure 2c). The lowest ^{13}C-CH_4 occurred with the highest CH_4 proportion was -52.5‰, which was about -5‰ higher than ^{13}C of dissolved CH_4 in surface water. It indicated that the lighter isotope of $^{12}CH_4$ is transported from water to air faster than $^{13}CH_4$. The negative linear relationship between CH_4 proportion and ^{13}C-CH_4 also suggested the variation of CH_4 was primarily caused by dilution of air with less CH_4 in the daytime (Figure 5k).

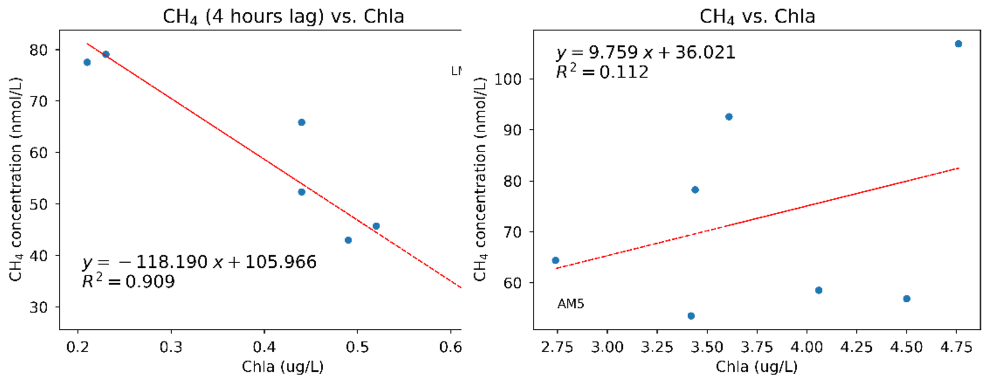

CH₄ (4 hours lag) vs. Chla
$y = -118.190\,x + 105.966$
$R^2 = 0.909$
CH₄ concentration (nmol/L)
Chla (ug/L)
CH₄ vs. Chla
$y = 9.759\,x + 36.021$
$R^2 = 0.112$
AM5
CH₄ concentration (nmol/L)
Chla (ug/L)

(a) (b)

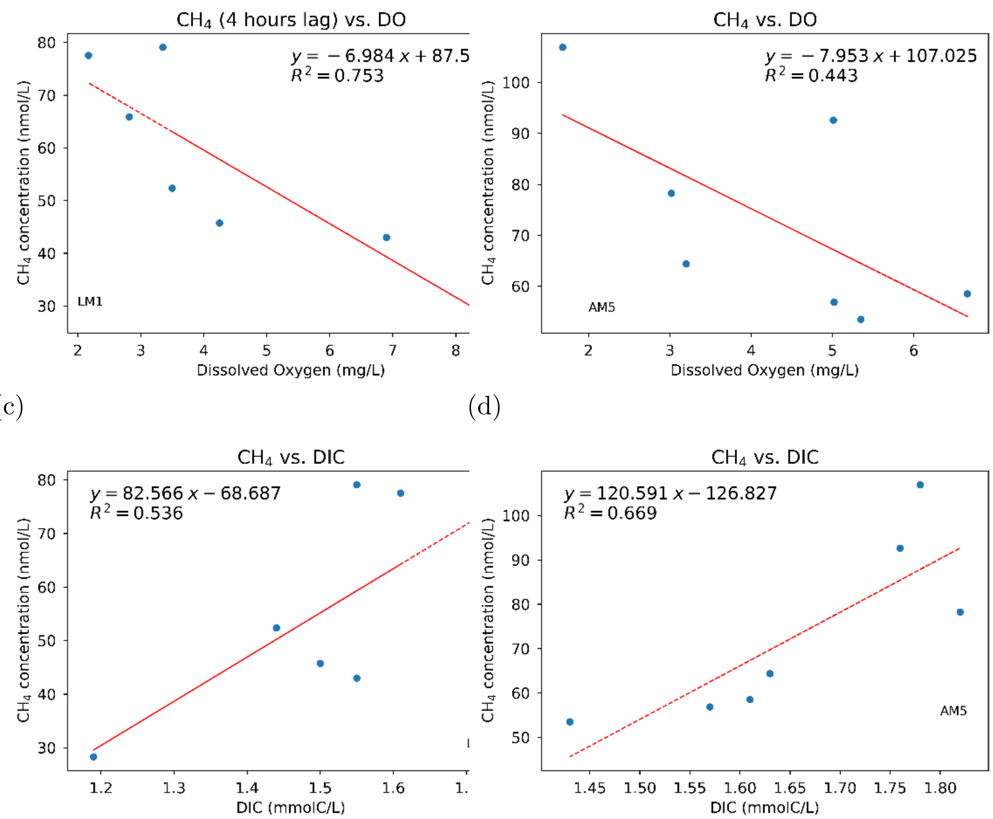

CH₄ (4 hours lag) vs. DO
$y = -6.984\,x + 87.5$
$R^2 = 0.753$
LM1
CH₄ concentration (nmol/L)
Dissolved Oxygen (mg/L)
CH₄ vs. DO
$y = -7.953\,x + 107.025$
$R^2 = 0.443$
AM5
CH₄ concentration (nmol/L)
Dissolved Oxygen (mg/L)
CH₄ vs. DIC
$y = 82.566\,x - 68.687$
$R^2 = 0.536$
CH₄ concentration (nmol/L)
DIC (mmolC/L)
CH₄ vs. DIC
$y = 120.591\,x - 126.827$
$R^2 = 0.669$
AM5
CH₄ concentration (nmol/L)
DIC (mmolC/L)

(c) (d)

(e) (f)

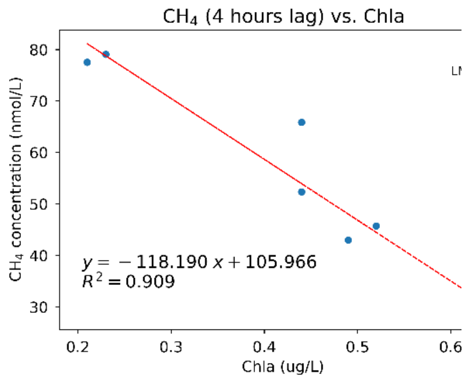

CH_4 (4 hours lag) vs. Chla
$y = -118.190\,x + 105.966$
$R^2 = 0.909$
Chla (ug/L)
CH_4 concentration (nmol/L)

(a)

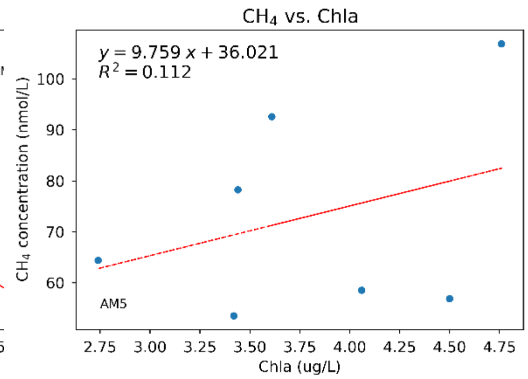

CH_4 vs. Chla
$y = 9.759\,x + 36.021$
$R^2 = 0.112$
AM5
Chla (ug/L)
CH_4 concentration (nmol/L)

(b)

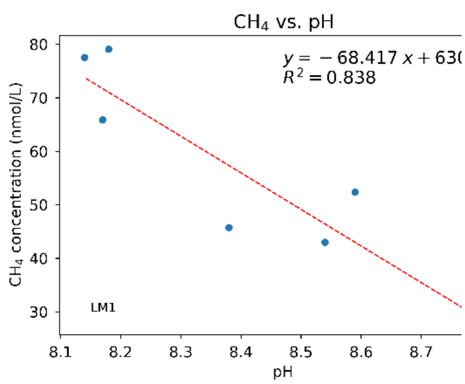

CH_4 vs. pH
$y = -68.417\,x + 63($
$R^2 = 0.838$
LM1
pH
CH_4 concentration (nmol/L)

(g)

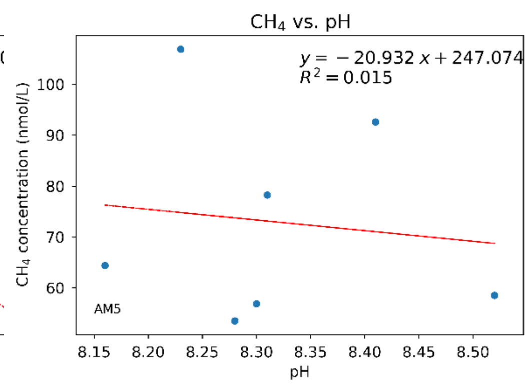

CH_4 vs. pH
$y = -20.932\,x + 247.074$
$R^2 = 0.015$
AM5
pH
CH_4 concentration (nmol/L)

(h)

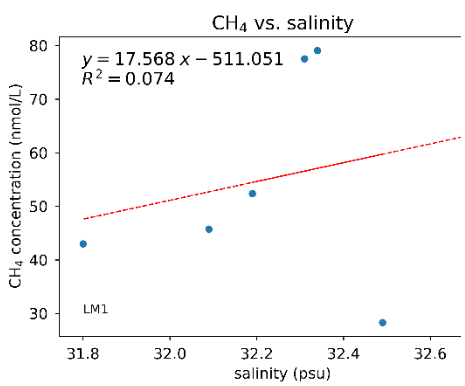

CH_4 vs. salinity
$y = 17.568\,x - 511.051$
$R^2 = 0.074$
LM1
salinity (psu)
CH_4 concentration (nmol/L)

(i)

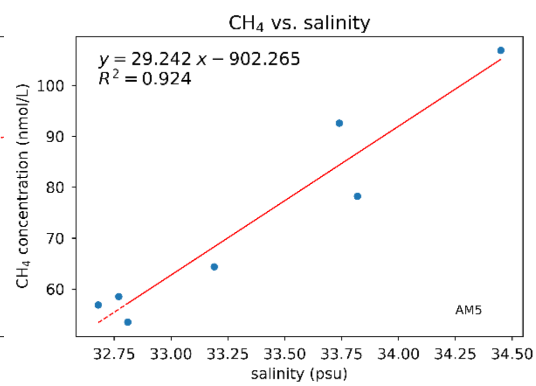

CH_4 vs. salinity
$y = 29.242\,x - 902.265$
$R^2 = 0.924$
AM5
salinity (psu)
CH_4 concentration (nmol/L)

(j)

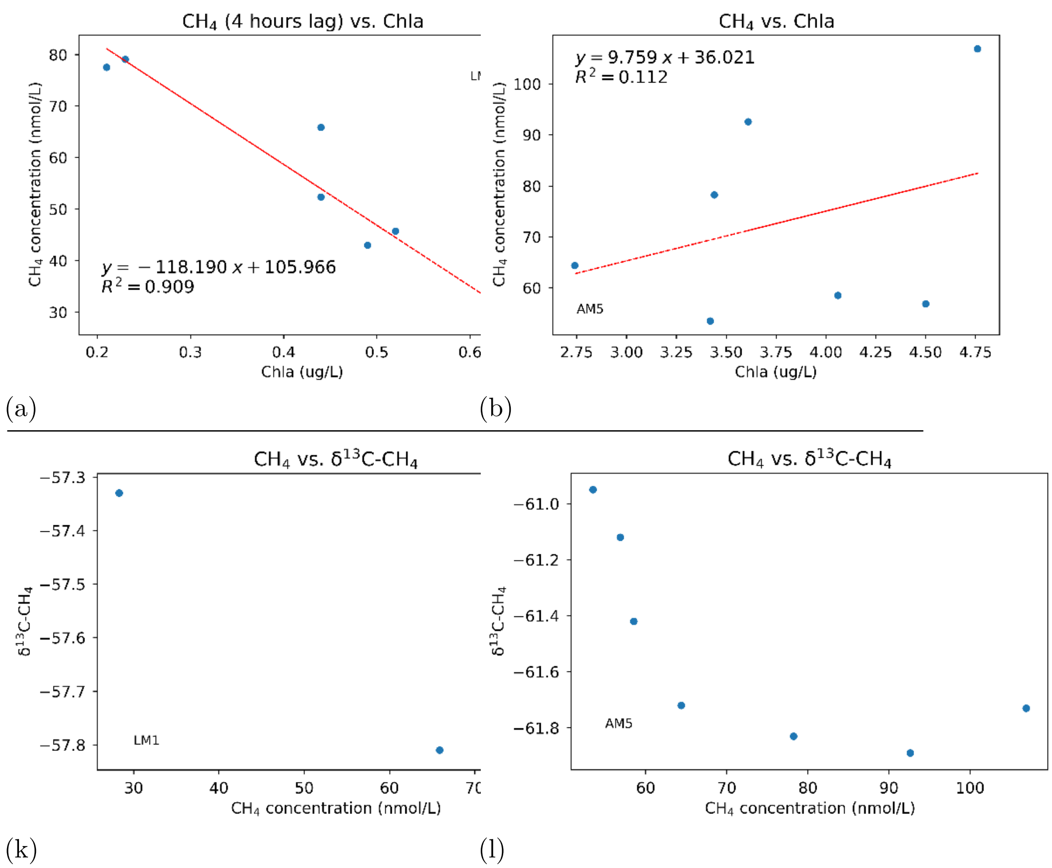

Figure 5. Relationship between dissolved CH_4 concentration and other parameters in the water column. Left: LM1; Right: AM5.

4.2.2 Sea-air CH_4 flux over the seagrass meadow

Unlike dissolved CH_4 concentration, sea-air CH_4 fluxes (Figure 2g) varied as wind speed changed. The CH_4 fluxes decreased as wind speed slowed down overnight, minimal before sunset when dissolved CH_4 concentration was maximum. CH_4 flux was significantly positively related to hourly wind speed (r^2=0.67, p<0.01), despite a difference between maximum and minimum CH_4 concentrations was nearly three times. It indicated the wind speed plays an essential role in releasing CH_4 from water to the atmosphere. Synchronically, CH_4 proportion in the ambient air was similar to sea-air CH_4, decreasing overnight. The decrease of CH_4 flux at the water-air interface in the nighttime further assisted the accumulation of dissolved CH_4 in the water column overnight.

Similarity between one-hour floating chamber flux and calculated diffusive CH_4

flux both in the daytime and nighttime further proved the impact of wind on CH_4 emission. In the long-term observation, CH_4 proportion did not increase linearly (Figure S1), which can be explained by variation in sea-air CH_4 fluxes. Total sea-air CH_4 flux in the whole day was calculated in four approaches (Table 1). The first one is the sum of diffusive CH_4 flux at different observation times multiplies duration between two observations. The other three were based on floating chamber fluxes. Extrapolation of one-hour fluxes of daytime and nighttime (0.174 $mmol/m^2 \cdot d$) was the largest. Since sea-air fluxes varied over time both in daytime and overnight and floating chamber flux did not change linearly, the extrapolation could bring large uncertainty. The flux (0.077 ± 0.012 $mmol/m^2 \cdot d$) acquired using the variation between final and initial CH_4 proportions in chambers was the smallest. And the other one got using the sum of variation of CH_4 proportion at different observation time was a bit larger (0.0895 $mmol/m^2 \cdot d$). Because of the weakness of static chambers applying in CH_4 flux measurement, these two fluxes are a rough estimation.

4.2.3 Dynamics of CH_4 cycling in seagrass meadow

The input and output of CH_4 generally decided dissolved CH_4 concentration in the water column. For seagrass meadow in this study, as in the previous discussion, the primary source of CH_4 was the CH_4 transported from sediment to water, and major output included CH_4 released from water to the air and CH_4 photo-oxidation by sunlight in water. Bacterial decomposition and production by methanogen in the water column were the minor sink and source of CH_4, respectively, based on the water incubation experiment. These factors were integrated into the following equations (equation 6-8) to estimate diurnal variation in CH_4 cycling. Since dissolved CH_4 was affected by photosynthetic and respiration processes of seagrass, sunlight decomposition was not considered in the night process (equation 7). Considering incubation of sediment and overlying water was carried out in sealed chambers, the impacts from limited DO, sunlight, and sea-air transport could be ignored (equation 8).

Daytime:

$$[CH_4]_{\text{remain}} = [CH_4]_{\text{sed-water}} - [CH_4]_{\text{oxidation}} + [CH_4]_{\text{methanogensis}} - [CH_4]_{\text{sea-air}} - [CH_4]_{\text{photo-oxidation}} \quad (6)$$

Night:

$$[CH_4]_{\text{remain}} = [CH_4]_{\text{sed-water}} - [CH_4]_{\text{oxidation}} + [CH_4]_{\text{methanogensis}} - [CH_4]_{\text{sea-air}} \quad (7)$$

Incubation:

$$[CH_4]_{\text{remain}} = [CH_4]_{\text{sed-water}} - [CH_4]_{\text{oxidation}} + [CH_4]_{\text{methanogensis}} \quad (8)$$

Here,

- $[CH_4]_{\text{remain}}$: dissolved CH_4 in the water column;

- $[CH_4]_{\text{sed-water}}$: CH_4 flux at the sediment-water interface;

- $[CH_4]_{\text{oxidation}}$: oxidization of CH_4 by bacteria in water;

- $[CH_4]_{\text{methanogensis}}$: methanogenesis of CH4 in water;

- $[CH_4]_{\text{photo-oxid}}$: photo-oxidation of CH_4 in water;

- $[CH_4]_{\text{sea-air}}$: CH_4 transported at the sea-air interface, determined by wind speed and dissolved CH_4 concentration.

An overall important assumption is that decomposition and production of CH_4 in the water body (-$[CH_4]_{\text{oxidation}}$ + $[CH_4]_{\text{methanogenesis}}$) in daytime and night are the same, which is less than 15% in one hour and less than 10% in 24 hours based on the incubation experiments (Figure S3). In the diurnal observation, the influence of wind speed was more significant than CH_4 concentration, and so daytime $[CH_4]_{\text{sea-air}}$ was larger than night $[CH_4]_{\text{sea-air}}$.

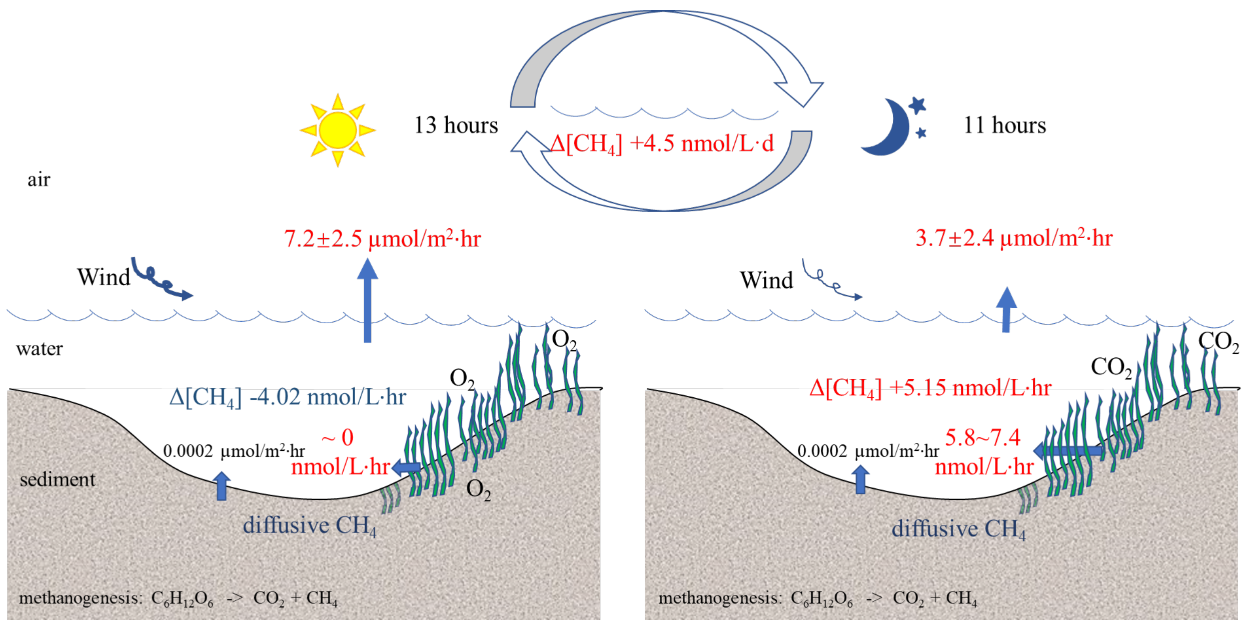

Figure 6. CH_4 cycling in the seagrass meadow. Left: daytime (13 hours); Right: nighttime (11 hours). CH_4 fluxes at the water-air interface were averages of diffusive fluxes in the daytime and nighttime respectively. Variation of CH_4 concentration in water body was calculated based on diurnal observation. Diffusive CH_4 flux at the sediment-water interface was calculated using the Fick's First Law (Table 1). Plant-mediation of CH_4 transport was calculated using variation of CH4 concentration in overlying water of sediment core. Detailed calculations see supplementary materials.

During 13 hours of daytime, dissolved CH_4 concentration decreased at an average -4.02 nmol/L · hr (Supplementary 2). On the contrary, dissolved CH_4

increased overnight (11 hours) with an hourly rate of +5.15 nmol/L · hr. The total daily variance was the sum of daytime decrease and night increase, that is, +4.5 nmol/L. There was 4.5 nmol/L of dissolved CH_4 accumulation each day in summer. However, 24-hour sediment incubation showed dissolved CH_4 concentration in overlying water increased 81.9 nmol/L. The difference between incubation and natural variances was 77.4 nmol/L, indicating 77.4 nmol/L dissolved CH_4 in water was consumed by photodecomposition and removed from water to air. Assuming average water depth in seagrass meadow was 1 m, 24-hour decrease of dissolved CH_4 would be 0.077 mmol/m^2 · d, which was similar to 24-hour floating chamber flux (0.077 ± 0.012 mmol/m^2 · d). Hence output of water column CH_4 was primarily emission from the water surface to the air. This point can further prove that the DO's impact worked more on sediment than the oxidation of CH_4 in the water column. Assuming oxygen in the chamber was enough to support seagrass photosynthesis and respiration during incubation, about 5.8 nmol/L · hr to 7.4 nmol/L · hr CH_4 was transported to water overnight. Calculated using elevated CH_4 concentration in overlying water and natural water, the turnover time of dissolved CH_4 in water was about 18 days.

4.2.4 Implication to seasonal variation

In other seasons, daytime hours decrease and night hours get longer. If we assume daytime decrease rate and nighttime increase rate keep the same as in this study, dissolved CH_4 remains in the water column after whole daily cycling would increase. However, since the primary increase of dissolved CH_4 came from seagrass transport from sediment, less biomass of seagrass in other seasons probably would deliver less CH_4 to the water column. Meanwhile, since wind speeds are lower in other seasons than in summer in this region, it would lead to less sea-air emission of CH_4. In all, remained CH_4 concentration in water ($[CH_4]_{remain}$) relies on the balance between sediment-water CH_4 flux ($[CH_4]_{sed\text{-}water}$) mediated by seagrass and transport of CH_4 from water to air ($[CH_4]_{sea\text{-}air}$). Therefore, seagrass biomass and wind speed in other seasons are probably crucial in determining the seasonal variation of dissolved CH_4 in seagrass water.

4.3 Mechanism of CH_4 transport in mangrove water

4.3.1 Impact of tidal process on CH_4 emission at mangrove

4.3.1.1 Tidal transport Unlike in seagrass (LM1), the diurnal variation of dissolved CH_4 concentration in mangrove/salt marsh areas (AM5) has a strong positive linear relationship with salinity, which seemed related to the tidal process. Moreover, CH_4 concentration and salinity variations were opposite with tidal water level (Figure 3b). During ebb, both CH_4 concentration and salinity increased, and during flooding, they decreased. Nevertheless, it is different with riverine estuaries, where CH_4 concentration increased during ebb due to riverine input with much higher dissolved CH_4 (Matoušů et al., 2017; Ye et al., 2019). Freshwater generally has a higher CH_4 concentration due to a less sulfate environment (DeLaune et al., 1983). Contrary to these studies, dissolved

CH_4 concentration at this mangrove site had a strong positive relationship with salinity (Figure 5j). Such variations in salinity and CH_4 concentration still can be explained by the tidal process.

Since AM5 is located in the middle of the mangrove creek, elevated salinity at midnight was caused by water transport with higher salinity from inside the mangrove water than evaporation. Because of high evaporation and less freshwater input (e.g., precipitation and riverine input) in summer, it is reasonable that shallower water inside the mangrove has a higher salinity than outside bay area. A decreasing salinity gradient (32.5, 32.1, 32.0, 31.5, respectively) from inside to outside along the creek, which has been observed one month before this observation (July 2019), can demonstrate this point (Figure S4).

Similarly, dissolved CH_4 concentration at AM5 was elevated during ebb due to tidal transport of water with a higher CH_4 level. Like the salinity, a dissolved CH_4 concentration gradient (109.7 nmol/L, 93.4 nmol/L, 72.5 nmol/L, 24.8 nmol/L, and 12.7 nmol/L, respectively) has been observed from inside to outside sites along this stream to the outlet of Ship Channel in July 2019 (Figure S4). Hence it is reasonable that CH_4 concentration at AM5 was elevated during the ebb and decreased during the flood. Moreover, CH_4 concentration increased from noon to evening and midnight, even when DO was high in the afternoon. It suggested quite limited CH_4 oxidation in the water column, that was agree with the water incubation experiment. Slightly decreased $^{13}C\text{-}CH_4$ during the ebb and elevated $^{13}C\text{-}CH_4$ in flooding manifested the input of biogenic CH_4 and dilution of bay water correspondingly. Unlike in seagrass, dissolved CH_4 was negatively related to in-situ DO rather than DO concentration several hours ago, further suggesting the transport of CH_4 by tidal current.

DO concentration was negatively corresponding with decrease in salinity. In the scenario without tidal influence, DO should continue to decrease after midnight until sunrise like DO variation at LM1. However, DO has increased since midnight as salinity decreased. It only could be explained by less input of saltier water with depleted DO and more transport of less salty water containing more DO. During flooding, tidal current from seaward with less salinity and higher DO diluted in-situ salinity and elevated DO concentration.

Although dissolved CH_4 was positively correlated to DIC, there was no relationship between dissolved CH_4 and pH. It suggested DIC and CH_4 were probably allochthonous, and the impact of photosynthesis on DIC was less significant. Moreover, as CH_4 concentration in the middle of the creek increased during the ebb, it meant CH_4 was being exported from the mangrove to the outside bay area, similar to observations in some other estuaries (Burgos et al., 2018).

4.3.1.2 Effect of tidal pumping Another tidal process that would control CH_4 cycling in the mangrove creek is the tidal pumping of porewater. It should note that the highest salinity and lowest DO did not synchronize with the lowest water level but occurred about a few hours in advance. It implied another water input at the end of the ebb. The highest CH_4 concentration also happened 4 hours before the lowest water level, further indicating water input with less dissolved CH_4 concentration to the water column. This observation could be explained by a contribution from sediment porewater by tidal pumping. CH_4 concentration in porewater at AM5 was about 40 nmol/L, less than that in the water column (diurnal variation: 53.5~106.9nmol/L). Hence, the dilution from porewater with less CH_4 could explain the reduction of dissolved CH_4 in 4 hours before the lowest water level, and tidally driven porewater exchange played a crucial role in this process. The transport of diffusive CH_4 at the sediment-water interface was generally passive and caused by a concentration gradient, expressed in Fick's First Law. Since sediment porewater CH_4 concentration was lower than that in the water body, passive delivery of CH_4 from sediment to water is minor. Therefore, only under the power of tidal pumping, as porewater was drawn to the overlying water, CH_4 in water column could be diluted by porewater. It is different from other mangrove creeks where porewater with high CH_4 concentration could increase CH_4 level in the water column (Burgos et al., 2018). That ^{13}C-CH_4 kept stable although CH_4 concentration decreased in the last few hours of ebb could prove that it was biogenic source input that caused the reducing CH_4 concentration before water level reached lowest.

Slightly elevated water temperature, pH, and DIC concentration at the lowest water level compared with 4 hours before CH_4 concentration and salinity were highest, all further suggested the input from sediment source. Dutta, et al. (2019) have found possible porewater influx of CO_2 during low tide in a mangrove-dominated tropical estuary in India (Dutta et al., 2019). The tidal pumping effect probably existed during all the ebb periods. However, the export from inside mangrove creek probably made this process negligible. When sufficient water has been exported near the end of ebb, tidal impact on sediment porewater could exhibit.

4.3.1.3 Tidal inundation From noon to evening during the diurnal observation, water depth had kept at a relatively high level for nearly eight hours since the end of flooding. Here takes this period as tidal inundation for discussion since the intertidal area was merged by water. The increase of CH_4 concentration began during this time. Notably, a few hours before ebb, CH_4 concentration increased significantly with a significant decrease of ^{13}C-CH_4 (Figure 2f), indicating more input of biogenic CH_4. It can be explained by tidal inundation of intertidal sediment, which could release additional CH_4 from intertidal porewater (Call et al., 2019).

Both the relationship between dissolved CH_4 concentration and CH_4 ^{13}C-CH_4 in water (Figure 5l) and that between CH_4 proportion and ^{13}C-CH_4 in the floating chamber (Figure 3f) showed, as more CH_4 was released from sediment to water, and from water to the chamber, ^{13}C-CH_4 decreased. It indicated the biogenic origin of CH_4 input. The trendline in Figure 3f represents the mixing process of initial atmospheric CH_4 and CH_4 entering the chamber from water. During the diurnal observation, ^{13}C of CH_4 emitted into the chamber from evening to the early morning was lower than the mixing process's data. It further suggested that the biogenic CH_4 came from sediment. Similarly, the relationship between dissolved CH_4 concentration and ^{13}C-CH_4 in the water column also looked like a hook (Figure 5l). It proved once more that not only the export of CH_4 from inside mangrove and dilution of CH_4 by bay water, but the input of biogenic CH_4 from sediment controlled the CH_4 variation in the mangrove creek.

4.3.2 Sea-air CH_4 flux in mangrove

Sea-air CH_4 fluxes acquired using floating chambers were much less than the calculated diffusive fluxes using the gas-transfer model, both in the daytime and at night (Figure 3g). The influence of wind speed could explain part of such discrepancy. Diffusive CH_4 fluxes were calculated using wind speed at 10 meters, while actual wind speed over the water surface was lower because of the barrier of mangrove vegetation. Different from AM5 surrounded by mangroves, seagrass site LM1 locates in open water. Thus, wind speeds over the water surface at LM1 could be compared with those at 10 meters. Wind speeds measured in the field about 1 meter above the water surface at LM1 were similar to data acquired at 10 meters, while one-meter wind speeds at AM5 were about 0.5 of those at 10 meters (Figure S5, $p<0.01$). Decreased gas exchange of diffusive CH_4 also has been reported in some macrophytes due to wind shelter (Attermeyer et al., 2016; Kosten et al., 2016). Hence it is reasonable that floating chamber flux was lower than calculated flux, and the floating chamber flux could reflect the actual transport at the water-air interface. When evaluating the diffusive CH_4 using the in-situ wind speeds, about a half of wind speeds used in the previous calculation, diffusive sea-air fluxes would be a quarter of previous results, similar to floating chamber fluxes.

The floating chamber flux in the evening (8 pm) was lower than that at noon (12 pm) due to lower wind speed, although dissolved CH_4 concentration was higher. Calculated diffusive CH_4 fluxes were also positively related to wind speeds rather than CH_4 concentration. Hence, although dissolved CH_4 concentration increased during the ebb, the ebb was not the process to emit more CH_4 to the atmosphere in this study, which is different from mangroves in some other areas (Jacotot et al., 2018).

Some studies have shown that tidal current could accelerate the emission of CH_4 in mangrove because turbulence caused by the tidal current in shallow water could raise the gas transfer velocity. The sea-air CH_4 fluxes in a mangrove creek in Australia calculated using four different empirical models, with or without considering tidal current, manifested that the addition of current velocity could get a higher CH_4 flux estimation (Call et al., 2015). The one-hour floating chamber fluxes at high tide (12 pm) and beginning of ebb (20 pm) were smaller than the calculated diffusive fluxes calculated using the model simply considering wind speed (Figure 3 and Figure 7), indicating no significant turbulent effect.

However, the chamber fluxes at the final few hours of ebb were similar to the calculated diffusive CH_4 (Figure 7). It probably could be attributed to the turbulence effect since wind impact further decreased as wind slowed down during that period. A study that applied floating chamber in six mangrove-dominated estuaries in Australia and the United States pointed out that the gas transfer velocities were highly temporal and spatial variable (Rosentreter et al., 2017). Our results further support this point.

4.3.3 Dynamics of CH_4 cycling in mangrove

Based on the above discussion, CH_4 transport along the creek included four stages (Figure 7) during this study's diurnal observation. CH_4 was produced and transported to the water column from sediment including upper inter-tidal sediment at an average of 4.5 nmol/L · hr in high tide. Then CH_4 produced inside the mangrove water was transported to the outside bay at 3.6 nmol/ L · hr during ebb. In the last four hours of ebb, tidal pumping's role became significant, drawing the porewater out of the sediment to dilute CH4 concentration in the water column. This process, combined with continuous export of CH_4, decreased CH_4 concentration at -7.2 nmol/L · hr. During the flood, bay water flushed into the mangrove along this creek and further diluted CH_4 concentration at AM5 at -3.5 nmol/L · hr. Bay water also could dilute porewater CH_4 concentration by flushing into the sediment through crabs' burrows or under pressure. When water inundated upper intertidal soil, water exchange probably could bring CH_4 out from deeper porewater, which often occurred during spring tides (Call et al., 2019). CH_4 fluxes in two floating chambers on intertidal sediment that suspended on the mud during the ebb and refloated during flood reached the rate of over 7 µmol/m^2 · hr. It indicated a potential input of ebullition CH_4 since the chamber fluxes were much higher than the diffusive flux. However, CH_4 proportion in the floating chamber that was away from intertidal sediment and always floating on the water decreased in the beginning few hours of flood and then increased significantly. It was probably related to the variation of dissolved CH_4, dilution by flooding bay water in the beginning and consequent increase due to intertidal sediment input. Although long-term chamber fluxes only could provide a rough estimation, it still manifested the complicated variation in CH_4 emission during the tidal process. The overall tidally variation in diffusive CH_4 concentration at AM5 was +1.6 nmol/L. Based on the increase of CH_4 concentration during high tide at AM5 and export of CH_4 via AM5, about 70% of CH_4 produced in mangrove sediment was exported to the outside bay during ebb. Therefore, tidal process could dramatically decrease the potential CH_4 emission to the atmosphere.

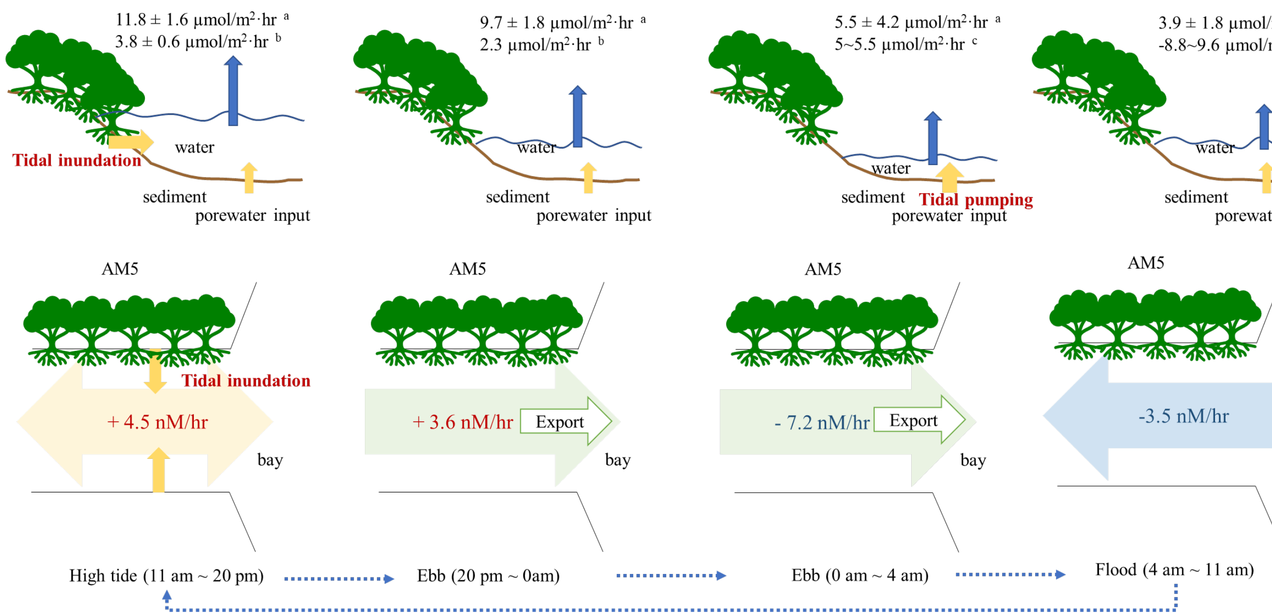

Figure 7. CH_4 cycling at the mangrove creek. Three periods were defined based on tidal procession (high tide, ebb and flood). Ebb was divided to two stages because tidal pumping was significant near the end of the ebb. [a] Diffusive flux calculated using the gas transfer model; [b] 1-hour floating chamber flux; [c] floating chamber flux based on the variation of CH_4 proportion between start and end of the corresponding period. +: increase; -: decrease.

This study showed less CH_4 emission in this mangrove site than in the seagrass site (Table 1, floating chamber fluxes). It primarily could be attributed to two factors, even though mangroves preserved more carbon in the sediment. First, wind sheltered by mangrove shrubs could decrease sea-air CH_4 emission. Second, during ebb, CH_4 could be transported to the outside bay area, which could further decrease the emission of CH_4 in mangrove water. Moreover, as CH_4 was diluted in open water, the saturation decreased, and consequently, less CH_4 can be released from the water surface to the air. During flooding, bay water with less CH_4 could dilute CH_4 in the creek and decrease CH_4 emission in mangrove water.

5. Conclusion

Diurnal variation of dissolved CH_4 concentration in seagrass meadow was positively correlated to DIC but was opposite to DO and Chl-*a* concentrations, indicating that the CH_4 cycling was related to photosynthesis and respiration of seagrass. Moreover, plant mediation played a vital role in CH_4 emission from sediment since the sediment-water diffusive CH_4 flux was minor. Unlike water associated with seagrass, the diurnal variation in CH_4 concentration in the mangrove creek was controlled by tidal processes. At the beginning of ebb, CH_4

was exported to the outside bay. However, in the last few hours of ebb, CH_4 concentration decreased because of the tidal pumping effect that brought porewater with less CH_4 concentration diluted CH_4 in the water column. During the flood, bay water with less CH_4 further diluted the CH_4 concentration in the creek. When tidal water merged upper intertidal sediment, tidal inundation could draw extra CH_4 from deeper porewater and elevated CH_4 concentration in water. Although the seagrass meadow and the mangrove creek locate at adjacent estuaries, their CH_4 emission from sediment to water was controlled by different mechanisms.

Sea-air CH_4 fluxes in these two areas showed different patterns with the CH_4 emission at the sediment-water interface. They followed a similar trend as wind speed. The peak fluxes appeared when wind speed was largest regardless of the dissolved CH_4 concentration. Diffusive CH_4 fluxes at the sea-air interface of seagrass were similar to floating chamber fluxes. In comparison, calculated diffusive CH_4 fluxes at the mangrove creek were larger than floating chamber fluxes except in the final hours of ebb. Such discrepancy was probably caused by lower wind speed over the water surface due to the sheltering of mangrove plants. Turbulent effect on CH_4 emission could become significant during ebb. It suggested that the diffusive CH_4 fluxes calculated using empirical models probably overestimated sea-air CH_4 flux at the mangrove creek. Floating chamber fluxes at seagrass and mangrove showed that more CH_4 was released from seagrass than from mangrove, which was different from other studies. Most studies investigated CH_4 released from mangrove and seagrass separately, while this project compared them directly since they locate at adjacent subtropical estuaries. Our results suggested that the contribution from subtropic seagrass to atmospheric CH_4 should get more concerned.

Moreover, the diurnal variation of CH_4 concentration in both regions probably further proved the common dilemma of greenhouse gas studies about when to sample during the day using the chamber-based method and discrete sampling (Bansal, 2018). However, understanding the dynamics of CH_4 cycling in different vegetation systems are significantly helpful in interpreting the data.

Acknowledgments

This work was finacially supported by an Institutional Grant (Grants-in-Aid of Graduate Research Program) to the Texas Sea Grant College Program from the NOAA, Texas A&M University-Corpus Christi Texas Comprehensive Research Funds, and Geological Society of America Graduate Student Grants. We are also very grateful to Dr. Paula Rose for her help in lab work and Mr. Chriss Shope for his help during sampling.

Data Availability Statement

Data for this research can be retrieved from Texas A&M University-Corpus Christi Repository (https://tamucc-ir.tdl.org/handle/1969.6/89674).

Reference

https://onlinelibrary.wiley.com/doi/abs/10.1111/gcb.15046

https://doi.org/10.1038/srep20424

https://doi.org/10.1007/s13157-018-1042-5

https://www.sciencedirect.com/science/article/pii/0016703796001585

https://doi.org/10.1007/s12237-017-0330-2

http://www.sciencedirect.com/science/article/pii/S0925857417305104

http://www.sciencedirect.com/science/article/pii/S0016703714007078

http://www.sciencedirect.com/science/article/pii/S0016703718307178

https://agupubs.onlinelibrary.wiley.com/doi/abs/10.1029/90JD01542

https://aslopubs.onlinelibrary.wiley.com/doi/abs/10.4319/lo.1969.14.3.0454

http://dx.doi.org/10.1111/j.1600-0889.1983.tb00002.x

https://onlinelibrary.wiley.com/doi/abs/10.1111/gcb.14430

http://www.sciencedirect.com/science/article/pii/S1002016007600575

https://www.cbbep.org/publications2/

http://www.sciencedirect.com/science/article/pii/S0272771419304792

http://www.sciencedirect.com/science/article/pii/S0304420314002370

https://www.frontiersin.org/article/10.3389/fmars.2017.00340

https://doi.org/10.1023/A:1006427712846

http://www.sciencedirect.com/science/article/pii/S0025326X1930712X

https://doi.org/10.1007/s00027-018-0580-5

http://www.sciencedirect.com/science/article/pii/S0048969718307617

https://nph.onlinelibrary.wiley.com/doi/abs/10.1111/nph.15995

https://doi.org/10.1023/B:BIOG.0000015277.17288.7a

https://www.sciencedirect.com/science/article/pii/S0043135416305681

https://doi.org/10.1093/aob/mcp201

http://www.sciencedirect.com/science/article/pii/S0022098100003002

https://doi.org/10.1007/s10533-017-0413-y

http://www.sciencedirect.com/science/article/pii/S0272771411004537

https://doi.org/10.1023/A:1005750201264

https://doi.org/10.1038/s41467-019-11693-w

https://doi.org/10.1007/s00027-016-0509-9 https://aslopubs.onlinelibrary.wiley.com/doi/abs/10.1002/lno.10953

http://www.sciencedirect.com/science/article/pii/S0304420399000134

https://aem.asm.org/content/aem/30/4/602.full.pdf

https://aslopubs.onlinelibrary.wiley.com/doi/abs/10.4319/lo.1977.22.3.0566

http://www.sciencedirect.com/science/article/pii/S0272771418301811

http://dx.doi.org/10.1021/cr050362v

https://doi.org/10.1007/s10498-011-9128-1

https://advances.sciencemag.org/content/advances/4/6/eaao4985.full.pdf

https://aslopubs.onlinelibrary.wiley.com/doi/abs/10.1002/lno.10444

https://essd.copernicus.org/articles/12/1561/2020/

https://doi.org/10.2307/1351568

https://agupubs.onlinelibrary.wiley.com/doi/abs/10.1029/2019JG005558

http://dx.doi.org/10.1029/92JC00188

https://aslopubs.onlinelibrary.wiley.com/doi/abs/10.4319/lom.2014.12.351

https://doi.org/10.1038/s41467-019-12541-7

https://agupubs.onlinelibrary.wiley.com/doi/abs/10.1029/92GB00710

https://www.sciencedirect.com/science/article/pii/0304377096010480

https://doi.org/10.1007/s10533-015-0085-4

https://doi.org/10.1007/s12237-017-0319-x

https://doi.org/10.1007/s13157-018-1015-8

https://aslopubs.onlinelibrary.wiley.com/doi/abs/10.1002/lno.10646

http://www.sciencedirect.com/science/article/pii/S0967064518301553

http://www.sciencedirect.com/science/article/pii/S0048969719314822

https://www.int-res.com/abstracts/meps/v173/p1-12/

Al-Haj, A. N., & Fulweiler, R. W. (2020). A synthesis of methane emissions from shallow vegetated coastal ecosystems. *Global Change Biology, 26*(5), 2988-3005. Armitage, A. R., Highfield, W. E., Brody, S. D., & Louchouarn, P. (2015). The contribution of mangrove expansion to salt marsh loss on the Texas Gulf Coast. *Plos One, 10*(5), e0125404. Attermeyer, K., Flury, S., Jayakumar, R., Fiener, P., Steger, K., Arya, V., et al. (2016). Invasive floating macrophytes reduce greenhouse gas emissions from a small tropical lake. *Scientific Reports, 6*(1), 20424. Bahlmann, E., Weinberg, I., Lavrič, J., Eckhardt, T., Michaelis, W., Santos, R., & Seifert, R. (2015). Tidal controls on trace gas dynamics in a seagrass meadow of the Ria Formosa lagoon (southern Portugal). *Biogeosciences,* *12*(6), 1683-1696. Bansal, S., Tangen, B., & Finocchiaro, R. (2018). Diurnal patterns of methane flux from a seasonal wetland: mechanisms and methodology. *Wetlands, 38*(5), 933-943. Berner, R. A. (1980). *Early diagenesis: a theoretical approach*: Princeton University Press.Bianchi, T. S., Allison, M. A., Zhao, J., Li, X. X., Comeaux, R. S., Feagin, R. A., & Kulawardhana, R. W. (2013). Historical reconstruction of mangrove expansion in the Gulf of Mexico: Linking climate change with carbon sequestration in coastal wetlands. *Estuarine Coastal and Shelf Science, 119*, 7-16. Borum, J., Sand-Jensen, K., Binzer, T., Pedersen, O., & Greve, T. M. (2007). Oxygen movement in seagrasses. In *Seagrasses: biology, ecologyand conservation* (pp. 255-270): Springer.Boudreau, B. P. (1996). The diffusive tortuosity of fine-grained unlithified sediments. *Geochimica et Cosmochimica Acta, 60*(16), 3139-3142. Broecker, W. S., & Peng, T.-H. (1974). Gas exchange rates between air and sea. *Tellus, 26*(1-2), 21-35. Burgos, M., Ortega, T., & Forja, J. (2018). Carbon dioxide and methane dynamics in Three Coastal Systems of Cadiz Bay (SW Spain). *Estuaries and Coasts, 41*(4), 1069-1088. Cabezas, A., Mitsch, W. J., MacDonnell, C., Zhang, L., Bydałek, F., & Lasso, A. (2018). Methane emissions from mangrove soils in hydrologically disturbed and reference mangrove tidal creeks in southwest Florida. *Ecological Engineering, 114*, 57-65. Call, M., Maher, D. T., Santos, I. R., Ruiz-Halpern, S., Mangion, P., Sanders, C. J., et al. (2015). Spatial and temporal variability of carbon dioxide and methane fluxes over semi-diurnal and spring–neap–spring timescales in a mangrove creek. *Geochimica et Cosmochimica Acta, 150*, 211-225. Call, M., Santos, I. R., Dittmar, T., de Rezende, C. E., Asp, N. E., & Maher, D. T. (2019). High pore-water derived CO_2 and CH_4 emissions from a macro-tidal mangrove creek in the Amazon region. *Geochimica et Cosmochimica Acta, 247*, 106-120. Chanton, J. P., Martens, C. S., Kelley, C. A., Crill, P. M., & Showers, W. J. (1992). Methane transport mechanisms and isotopic fractionation in emergent macrophytes of an Alaskan tundra lake. *Journal of Geophysical Research: Atmospheres, 97*(D15), 16681-16688. Chuang, P. C., Young, M. B., Dale, A. W., Miller, L. G., Herrera-Silveira, J. A., & Paytan, A. (2017). Methane fluxes from tropical coastal lagoons surrounded by mangroves, Yucatan, Mexico. *Journal of Geophysical Research-Biogeosciences, 122*(5), 1156-1174. Cline, J. D. (1969). Spectrophotometric determination of hydrogen sulfide in natural waters. *Limnology and Oceanography, 14*(3), 454-458. Coffin, R. B., Smith, J. P., Plummer, R. E., Yoza, B., Larsen, R. K., Millholland, L. C., & Montgomery, M. T. (2013). Spatial variation in shallow sediment methane sources and cycling on the Alaskan Beaufort Sea Shelf/Slope. *Marine and Petroleum Geology, 45*, 186-197. DeLaune, R. D., Smith, C. J., & Patrick, W. H. (1983). Methane release from Gulf coast wetlands. *Tellus B, 35B*(1), 8-15. Diefenderfer, H. L., Cullinan, V. I., Borde, A. B., Gunn, C. M., & Thom, R. M. (2018). High-frequency greenhouse gas flux measurement system detects winter storm surge effects on salt marsh. *Global Change Biology, 24*(12), 5961-5971. Ding, W.-X., & Cai, Z.-C. (2007). Methane emission from natural wetlands in China: summary of years 1995–2004 Studies. *Pedosphere, 17*(4), 475-486. Dunton, K. H., & Reyna, N. E. (2019). *A long-term seagrass monitoring program for Corpus Christi Bay and Upper Laguna Madre.* Retrieved from Coastal

Bend Bays and Estuaries Program: Dutta, M. K., Kumar, S., Mukherjee, R., Sharma, N., Acharya, A., Sanyal, P., et al. (2019). Diurnal carbon dynamics in a mangrove-dominated tropical estuary (Sundarbans, India). *Estuarine, Coastal and Shelf Science, 229*, 106426. Dutta, M. K., Mukherjee, R., Jana, T. K., & Mukhopadhyay, S. K. (2015). Biogeochemical dynamics of exogenous methane in an estuary associated to a mangrove biosphere; The Sundarbans, NE coast of India. *Marine Chemistry, 170*, 1-10. Fonseca, A. L. D., Marinho, C. C., & Esteves, F. D. (2017). Floating Aquatic Macrophytes Decrease the methane concentration in the water column of a tropical coastal lagoon: Implications for methane oxidation and emission. *Brazilian Archives of Biology and Technology, 60*, 16. Garcias-Bonet, N., & Duarte, C. M. (2017). Methane production by seagrass ecosystems in the Red Sea. *Frontiers in Marine Science, 4*(340). Original Research. Heilman, M. A., & Carlton, R. G. (2001). Methane oxidation associated with submersed vascular macrophytes and its impact on plant diffusive methane flux. *Biogeochemistry, 52*(2), 207-224. Huang, C.-M., Yuan, C.-S., Yang, W.-B., & Yang, L. (2019). Temporal variations of greenhouse gas emissions and carbon sequestration and stock from a tidal constructed mangrove wetland. *Marine Pollution Bulletin, 149*, 110568. Huertas, I. E., Flecha, S., Navarro, G., Perez, F. F., & de la Paz, M. (2018). Spatio-temporal variability and controls on methane and nitrous oxide in the Guadalquivir Estuary, Southwestern Europe. *Aquatic Sciences, 80*(3), 29. Jacotot, A., Marchand, C., & Allenbach, M. (2018). Tidal variability of CO_2 and CH_4 emissions from the water column within a Rhizophora mangrove forest (New Caledonia). *Science of the Total Environment, 631-632*, 334-340. Jeffrey, L. C., Reithmaier, G., Sippo, J. Z., Johnston, S. G., Tait, D. R., Harada, Y., & Maher, D. T. (2019). Are methane emissions from mangrove stems a cryptic carbon loss pathway? Insights from a catastrophic forest mortality. *New Phytologist, 224*(1), 146-154. Jha, C. S., Rodda, S. R., Thumaty, K. C., Raha, A., & Dadhwal, V. K. (2014). Eddy covariance based methane flux in Sundarbans mangroves, India. *Journal of Earth System Science, 123*(5), 1089-1096. Kankaala, P., & Bergström, I. (2004). Emission and oxidation of methane in Equisetum fluviatile stands growing on organic sediment and sand bottoms. *Biogeochemistry, 67*(1), 21-37. Kosten, S., Piñeiro, M., de Goede, E., de Klein, J., Lamers, L. P. M., & Ettwig, K. (2016). Fate of methane in aquatic systems dominated by free-floating plants. *Water Research, 104*, 200-207. Laanbroek, H. J. (2009). Methane emission from natural wetlands: interplay between emergent macrophytes and soil microbial processes. A mini-review. *Annals of Botany, 105*(1), 141-153. Lee, K.-S., & Dunton, K. H. (2000). Diurnal changes in pore water sulfide concentrations in the seagrass *Thalassia testudinum* beds: the effects of seagrasses on sulfide dynamics. *Journal of Experimental Marine Biology and Ecology, 255*(2), 201-214. Li, H., Dai, S., Ouyang, Z., Xie, X., Guo, H., Gu, C., et al. (2018). Multi-scale temporal variation of methane flux and its controls in a subtropical tidal salt marsh in eastern China. *Biogeochemistry, 137*(1), 163-179. Livesley, S. J., & Andrusiak, S. M. (2012). Temperate mangrove and salt marsh sediments are a small methane and nitrous oxide source but important carbon store. *Estuarine, Coastal and Shelf Science, 97*, 19-27. Lombardi, J. E., Epp,

M. A., & Chanton, J. P. (1997). Investigation of the methyl fluoride technique for determining rhizospheric methane oxidation. *Biogeochemistry, 36*(2), 153-172. Lorenson, T. D., Grienert, J., & Coffin, R. B. (2016). Dissolved methane in the Beaufort Sea and the Arctic Ocean, 1992-2009; sources and atmospheric flux. *Limnology and Oceanography, 61*, S300-S323. Macreadie, P. I., Anton, A., Raven, J. A., Beaumont, N., Connolly, R. M., Friess, D. A., et al. (2019). The future of Blue Carbon science. *Nature Communications, 10*(1), 3998. Magen, C., Lapham, L. L., Pohlman, J. W., Marshall, K., Bosman, S., Casso, M., & Chanton, J. P. (2014). A simple headspace equilibration method for measuring dissolved methane. *Limnology and Oceanography-Methods, 12*, 637-650. Matoušů, A., Osudar, R., Šimek, K., & Bussmann, I. (2017). Methane distribution and methane oxidation in the water column of the Elbe estuary, Germany. *Aquatic Sciences, 79*(3), 443-458. Montagna, P. A., Brenner, J., Gibeaut, J., & Morehead, S. (2011). Coastal impacts. In J. Schmandt, G. R. North, & J. Clarkson (Eds.), *The impact of global warming on Texas* (pp. 96-123). Texas: University of Texas Press.Montagna, P. A., Hu, X., Palmer, T. A., & Wetz, M. (2018). Effect of hydrological variability on the biogeochemistry of estuaries across a regional climatic gradient. *Limnology and Oceanography, 63*(6), 2465-2478. Morin, J., & Morse, J. W. (1999). Ammonium release from resuspended sediments in the Laguna Madre estuary. *Marine Chemistry, 65*(1), 97-110. Oremland, R. S. (1975). Methane production in shallow-water, tropical marine sediments. *Applied Microbiology, 30*(4), 602-608. Oremland, R. S., & Taylor, B. F. (1977). Diurnal fluctuations of O_2, N_2, and CH_4 in the rhizosphere of *Thalassia testudinum. Limnology and Oceanography, 22*(3), 566-570. Osland, M. J., Feher, L. C., López-Portillo, J., Day, R. H., Suman, D. O., Guzmán Menéndez, J. M., & Rivera-Monroy, V. H. (2018). Mangrove forests in a rapidly changing world: Global change impacts and conservation opportunities along the Gulf of Mexico coast. *Estuarine, Coastal and Shelf Science, 214*, 120-140. Reeburgh, W. S. (2007). Oceanic methane biogeochemistry. *Chemical Reviews, 107*(2), 486-513. Reese, B. K., Finneran, D. W., Mills, H. J., Zhu, M.-X., & Morse, J. W. (2011). Examination and refinement of the determination of aqueous hydrogen sulfide by the methylene blue method. *Aquatic Geochemistry, 17*(4), 567. Rosentreter, J. A., Maher, D. T., Erler, D. V., Murray, R. H., & Eyre, B. D. (2018). Methane emissions partially offset "blue carbon" burial in mangroves. *Science Advances, 4*(6), eaao4985. Rosentreter, J. A., Maher, D. T., Ho, D. T., Call, M., Barr, J. G., & Eyre, B. D. (2017). Spatial and temporal variability of CO_2 and CH_4 gas transfer velocities and quantification of the CH_4 microbubble flux in mangrove dominated estuaries. *Limnology and Oceanography, 62*(2), 561-578. Saunois, M., Stavert, A. R., Poulter, B., Bousquet, P., Canadell, J. G., Jackson, R. B., et al. (2020). The global methane budget 2000–2017. *Earth Syst. Sci. Data, 12*(3), 1561-1623. Smith, N. P. (1979). Tidal dynamics and low-frequency exchanges in the Aransas Pass, Texas. *Estuaries, 2*(4), 218-227. Trifunovic, B., Vázquez-Lule, A., Capooci, M., Seyfferth, A. L., Moffat, C., & Vargas, R. (2020). Carbon dioxide and methane emissions from a temperate salt marsh tidal creek. *Journal of Geophysical Research: Biogeosciences, 125*(8), e2019JG005558. Wanninkhof, R. (1992). Relationship between wind speed and gas exchange over the ocean. *Journal of Geophysical Research: Oceans, 97*(C5), 7373-7382. Wanninkhof, R. (2014). Relationship between wind speed and gas exchange over the ocean revisited. *Limnology and Oceanography: Methods, 12*(6), 351-362. Weber, T., Wiseman, N. A., & Kock, A. (2019). Global ocean methane emissions dominated by shallow coastal waters. *Nature Communications, 10*(1), 4584. Whiting, G. J., & Chanton, J. P. (1992). Plant-dependent CH_4 emission in a subarctic Canadian fen. *Global Biogeochemical Cycles, 6*(3), 225-231. Whiting, G. J., & Chanton, J. P. (1996). Control of the diurnal pattern of methane emission from emergent aquatic macrophytes by gas transport mechanisms. *Aquatic Botany, 54*(2), 237-253. Wiesenburg, D. A., & Guinasso, N. L. (1979). Equilibrium solubilities of methane, carbon monoxide, and hydrogen in water and sea water. *Journal of Chemical and Engineering Data, 24*(4), 356-360. Wilson, B. J., Mortazavi, B., & Kiene, R. P. (2015). Spatial and temporal variability in carbon dioxide and methane exchange at three coastal marshes along a salinity gradient in a northern Gulf of Mexico estuary. *Biogeochemistry, 123*(3), 329-347. journal article. Wilson, S. S., & Dunton, K. H. (2018). Hypersalinity during regional drought drives mass mortality of the seagrass *Syringodium filiforme* in a subtropical lagoon. *Estuaries and Coasts, 41*(3), 855-865. Yang, W.-B., Yuan, C.-S., Huang, B.-Q., Tong, C., & Yang, L. (2018). Emission characteristics of greenhouse gases and their correlation with water quality at an estuarine mangrove ecosystem – the application of an in-situ on-site NDIR monitoring technique. *Wetlands, 38*(4), 723-738. Yao, H., & Hu, X. (2017). Responses of carbonate system and CO_2 flux to extended drought and intense flooding in a semiarid subtropical estuary. *Limnology and Oceanography, 62*(S1), S112-S130. Ye, W., Zhang, G., Zheng, W., Zhang, H., & Wu, Y. (2019). Methane distributions and sea-to-air fluxes in the Pearl River Estuary and the northern South China sea. *Deep Sea Research Part II: Topical Studies in Oceanography, 167*, 34-45. Zhang, M., Xiao, Q., Zhang, Z., Gao, Y., Zhao, J., Pu, Y., et al. (2019). Methane flux dynamics in a submerged aquatic vegetation zone in a subtropical lake. *Science of the Total Environment, 672*, 400-409. Ziegler, S., & Benner, R. (1998). Ecosystem metabolism in a subtropical, seagrass-dominated lagoon. *Marine Ecology Progress Series, 173*, 1-12.